

Involvement of the neck coiled-coil in the velocity of UNC104, a kinesin-related motor protein
by Marcia Rebecca Kary

A thesis submitted in partial fulfillment of the requirements for the degree of Master of Science in Biochemistry
Montana State University
© Copyright by Marcia Rebecca Kary (2001)

Abstract:
There is considerable debate over the mechanism of motility for kinesin-related proteins. Dimeric motors, such as conventional kinesin, are believed to translocate along microtubules in a hand-over-hand fashion. Some members of the UNC104/KIF1 subfamily maybe monomeric, however, and therefore the mechanism of motility would differ. It is hypothesized that the monomers may operate with a lever-arm mechanism, analogous to myosin. Conventional kinesin and UNC-104 quaternary structures have regions of coiled-coils. In UNC-104 the coiled-coils are found in the neck region, while for conventional kinesin they are found throughout the neck and stalk domain. Coiled-coils are responsible for the dimerization of conventional kinesin. The coiled-coils found in UNC-104 are conserved throughout the subfamily. Since UNC-104 is likely monomeric, the conserved coiled-coils may have another function. Current studies have linked the neck coiled-coil to motor velocity.

This research addresses the possible involvement of the monomeric neck coiled-coil in motor velocity. Specifically, we addressed the possibility of intramolecular coiled-coil formation, resulting in a stiff lever arm, which mediates motor motility. Various neck region truncations of UNC-104 were recombinantly expressed and purified and applied to in vitro microtubule motility assays. The motor velocities were analyzed using a Nikon microscope equipped with differential interference contrast optics.

Three constructs were made; U345/GFP, U360/GFP, and U380/GFP. U345/GFP did not contain the neck linker and showed no movement. U360/GFP and U380/GFP displayed similar velocities, with truncations before the neck coiled-coil and after the neck coiled-coil, respectively.

Neck truncations before and after the neck coiled-coil had an insignificant effect on motor velocity. Alternatively, the elimination of the neck linker had a severe effect on motor velocity, similar to results found for conventional kinesin. These results argue against the possibility of a lever arm, leaving open the possibility that UNC-104 and dimeric conventional kinesin have similar motility mechanisms.

INVOLVEMENT OF THE NECK COILED-COIL IN THE VELOCITY OF UNC104, A KINESIN-RELATED MOTOR PROTEIN

by

Marcia Rebecca Kary

A thesis submitted in partial fulfillment
of the requirements for the degree

of

Master of Science

In

Biochemistry

MONTANA STATE UNIVERSITY
Bozeman, Montana

April 2001

N378
K1499

APPROVAL

of a thesis submitted by

Marcia Rebecca Kary

This thesis has been read by each member of the thesis committee and has been found to be satisfactory regarding content, English usage, format, citations, bibliographic style, and consistency, and is ready for submission to the College of Graduate Studies.

Dr. Daniel W. Pierce _____ 4/23/2001
(Signature) Date

Approved for the Department of Chemistry and Biochemistry

Dr. Paul A. Grieco _____ 4/23/01
(Signature) Date

Approved for the College of Graduate Studies

Dr. Bruce R. McLeod _____ 4-23-01
(Signature) Date

STATEMENT OF PERMISSION TO USE

In presenting this thesis in partial fulfillment of the requirements for a master's degree at Montana State University, I agree that the Library shall make it available to borrowers under rules of the Library.

If I have indicated my intention to copyright this thesis by including a copyright notice page, copying is allowable only for scholarly purposes, consistent with "fair use" as prescribed in the U.S. Copyright Law. Requests for permission for extended quotation from or reproduction of this thesis in whole or in parts may be granted only by the copyright holder.

Signature 

Date 4/23/07

I dedicate this thesis to my faithful companion Miss Cleopatra, who passed away before seeing me finish. She purred by me during four years of high school, four years of college, two years off, and almost made it the full four years of graduate school. There will be something missing when I receive my degree. I love you kiki.

Thank you daddy for letting me keep her.

I would like to thank everyone who talked me into sticking it out and not walking away. I would like to thank my son, Elijah, for all the smiling faces, hugs and kisses. They got me through some pretty tough days. I would like to thank my daddy, for giving the gift of self-motivation and strong-will. I would like to thank my mommy, for having a mother's heart and loving me when I needed it most. I would like to thank my brother and sisters, for helping me through some very difficult times. I would like to thank Dana, without you I don't know where I would be now, thanks for the constant support. I would like to thank Mark, for his friendship, concern and love. I would like to thank my advisor, for giving me an exciting project to work on. Lastly, I would like to thank Alex and Absarokee, for their wagging tails everyday when I got home from school. I love you all. What can I say, I made it and with out each of you I would not have. God Bless You.

TABLE OF CONTENTS

1. BACKGROUND.....1

Cytoskeletal Motor Proteins.....1
Conventional Kinesin.....5
Monomeric Kinesin UNC104/KIF1 Subfamily.....18

2. INTRODUCTION.....25

3. MATERIALS AND METHODS.....28

Plasmid Construction.....28
Protein Expression and Purification.....29
Microtubule Affinity Purification.....31
Microtubule Gliding Assays.....33
Perfusion Chamber Construction.....33
Generation of Long Microtubules.....33
Gliding Assays.....34

4. RESULTS.....37

Protein Expression and Purification.....37
Microtubule Gliding Assays.....40

5. DISCUSSION.....52

6. SUMMARY.....60

7. REFERENCES CITED.....61

LIST OF TABLES

Table Page

1. Comparison of Various Neck Truncations on UNC-104 Velocity....41
2. Velocities Displayed by 653/GFP....42
3. Velocities Displayed by U360/GFP....45
4. Velocities Displayed by U360/GFP....46
5. Velocities Displayed by U360/GFP....47
6. Velocities Displayed by U380/GFP....49
7. Velocities Displayed by U380/GFP....50

LIST OF FIGURES

Figure Page

1. Organization of Microtubule Subunits....3
2. Conventional Kinesin Heavy Chain Dimer....6
3. Crystal Structure of Dimeric Rat Conventional Kinesin....9
4. Kinesin Superfamily Quaternary Structures....13
5. Coiled-Coil Prediction of Conventional Kinesin....16
6. Coiled-Coil Prediction of UNC-104....17
7. UNC104/KIF1 Subfamily Coiled-Coil Prediction....20
8. Conserved Regions in Monomeric UNC-104....23
9. Kinesin Catalyzed Movement of Microtubules....35
10. DIC Image of Microtubules....35
11. Protein Purification SDS-PAGE Gels....38
12. Western Detection for GFP Fusion Protein....39
13. Microtubule Affinity Purification SDS-PAGE Gels....39
14. UNC-104 Velocities Achieved with Various Neck Truncations....41
15. Velocities Displayed by U653/GFP....43
16. Velocities Displayed by U360/GFP....48
17. Velocities Displayed by U380/GFP....51

LIST OF FIGURES

Figure Page

18. Schematic of UNC-104 Constructs.....55

ABSTRACT

There is considerable debate over the mechanism of motility for kinesin-related proteins. Dimeric motors, such as conventional kinesin, are believed to translocate along microtubules in a hand-over-hand fashion. Some members of the UNC104/KIF1 subfamily maybe monomeric, however, and therefore the mechanism of motility would differ. It is hypothesized that the monomers may operate with a lever-arm mechanism, analogous to myosin. Conventional kinesin and UNC-104 quaternary structures have regions of coiled-coils. In UNC-104 the coiled-coils are found in the neck region, while for conventional kinesin they are found throughout the neck and stalk domain. Coiled-coils are responsible for the dimerization of conventional kinesin. The coiled-coils found in UNC-104 are conserved throughout the subfamily. Since UNC-104 is likely monomeric, the conserved coiled-coils may have another function. Current studies have linked the neck coiled-coil to motor velocity.

This research addresses the possible involvement of the monomeric neck coiled-coil in motor velocity. Specifically, we addressed the possibility of intramolecular coiled-coil formation, resulting in a stiff lever arm, which mediates motor motility. Various neck region truncations of UNC-104 were recombinantly expressed and purified and applied to *in vitro* microtubule motility assays. The motor velocities were analyzed using a Nikon microscope equipped with differential interference contrast optics.

Three constructs were made; U345/GFP, U360/GFP, and U380/GFP. U345/GFP did not contain the neck linker and showed no movement. U360/GFP and U380/GFP displayed similar velocities, with truncations before the neck coiled-coil and after the neck coiled-coil, respectively.

Neck truncations before and after the neck coiled-coil had an insignificant effect on motor velocity. Alternatively, the elimination of the neck linker had a severe effect on motor velocity, similar to results found for conventional kinesin. These results argue against the possibility of a lever arm, leaving open the possibility that UNC-104 and dimeric conventional kinesin have similar motility mechanisms.

CHAPTER 1

BACKGROUND

Cytoskeletal Motor Proteins

The early hypothesis that transport of materials in cells was accomplished by diffusion is very distant from our current understanding. It is now known that cellular transport of materials is primarily accomplished by cytoskeletal motor proteins. Motor proteins attach to cargoes and move them to various locations in the cell. Vesicular organelle transport, flagellar beating, axonal transport, chromosome segregation, and muscle contraction are a few of the motility processes motor proteins perform (Goldstein, 1993). The mechanisms by which motors interact with and move their cargoes are poorly understood.

Cytoskeletal motor proteins use the chemical energy of ATP hydrolysis to generate force and movement along cytoskeletal filaments (Vale and Fletterick, 1997). The three major types of cytoskeletal filaments are f-actin, microtubules, and intermediate filaments. Actin and microtubules are polar polymers of filament-forming proteins with kinetically and structurally distinct "plus" and "minus" ends (Microtubule interactions, http://blocks.fhcrc.org/~kinesin.html). This polarity enables the directional movement of the motor proteins.

Intermediate filaments are not polar (Goldstein, 1993), and hence are not believed to support cellular transport by motor proteins. There are three superfamilies of motor proteins, the kinesins, dyneins, and myosins. Kinesins and dyneins travel along microtubules, while myosin travels along actin filaments (Goldstein, 1993). Actin filaments and microtubules are both involved in the generation of internal cellular movements and structures as well as cellular attachment to and movement on substrates. Actin filaments, for example, participate in the contraction of muscle and unconventional myosin motors are known to transport vesicular cargo along actin filaments (Discovery of Acanthamoeba Myosin-I, the First Unconventional Myosin, http://blocks.fhcrc.org/~kinesin.html). Microtubules are the main structural and force-generating elements in cilia and flagella and form the frameworks of meiotic and mitotic spindles. They additionally participate in organization of the cytoplasm, where in non-dividing cells they align the nucleus, endoplasmic reticulum, Golgi apparatus, and possibly other organelles.

Microtubules are polymerized from specific nucleating complexes within the centrosome. Most microtubules remain attached to the centrosome, but some are released and transported to specific sites within the cell body (Hoenger *et al.*, 1998). Microtubules have two stages of formation; nucleation and elongation. During "nucleation", α/β tubulin heterodimers associate by both lateral and end-to-end interactions to form a fragment of a microtubule (Figure 1). While this process occurs spontaneously *in vitro* in solutions containing purified tubulin at

Figure 1:
Organization of Microtubule Subunits

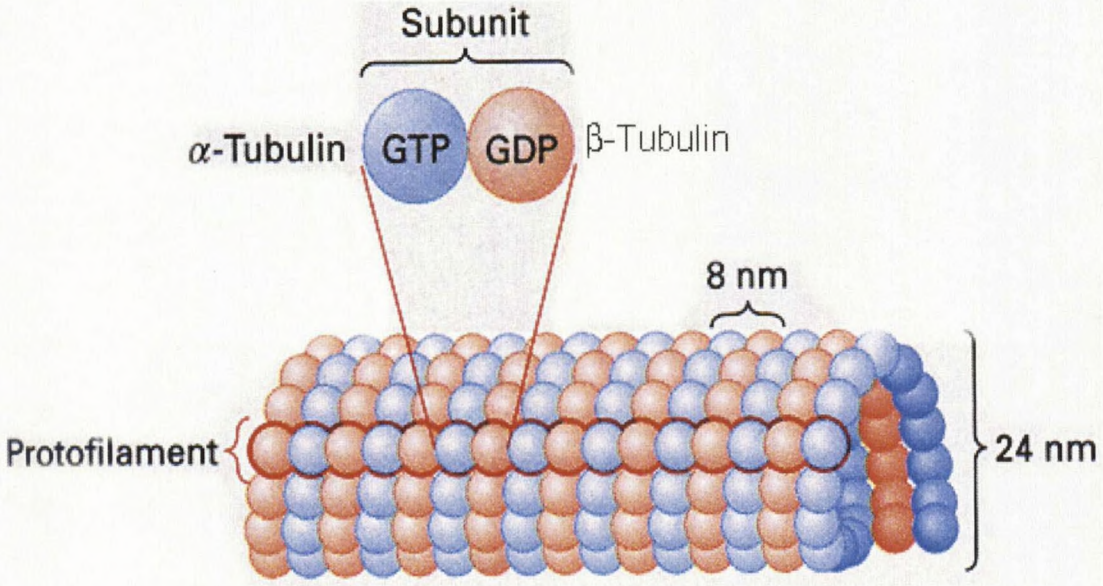


Figure1:
The organization of α/β tubulin subunits, or dimers, in a microtubule. Each dimer measures 8nm in length. Microtubule formation involves the stacking of tubulin dimers end to end, which form a protofilament. The protofilaments are packed side by side, forming the walls of the microtubule.
(Song & Mandelkow, 1993)

high concentrations, in the cell most microtubules are nucleated by a specific centrosomal complex (the γ-TuRC ring complex) that caps the microtubule minus end and thus causes a microtubule array to form in which the plus ends are distal. Microtubules that release from the centrosome are generally transported with their positive ends leading; thus maintaining the plus-end-distal polarity orientation within the cell (Wang *et al.*, 1996). Structurally, microtubules are composed of 13 protofilaments that associate laterally to form a hollow cylinder, with the protofilaments running parallel to the cylinder axis. Each protofilament is a string of α/β tubulin heterodimers. While 13 protofilaments microtubules are more typical, microtubules with 12 to 16 protofilaments have been observed in various organisms and cell types (Goldstein, 1993).

Movement of motor proteins along microtubules is unidirectional. All known dynein motors have minus-end directed movement. Most kinesin motors have plus-end directed movement, although there are some exceptions such as the minus-end directed kinesin Ncd (McDonald *et al.*, 1990).

Motor proteins have a role in many cell biological processes. Because of this, there is much interest in the research their mechanisms and cellular functions. Current studies have proven that motor proteins are linked to diseases. Familial amyotrophic lateral sclerosis (FALS) is a neurodegenerative disease that affects middle-aged people (Dupuis *et al.*, 2000). This disease involves the accumulation of neurofilament proteins, which impairs axonal transport by retarding motor protein movement. With the onset of this disease there is an

increase in the expression of KAP3, a non-motor KIF3A associated subunit. This compensatory mechanism delays the degenerative process by sustaining part of axonal transport through increased motor availability. These findings compound the need for a further understanding of kinesin structure and function.

In the 1960's dynein was discovered in cilia and in the 1980's the first kinesin (now called conventional kinesin) was isolated from squid giant axons, sea urchin eggs, and chick brain (Brady, 1985; Scholey *et al.*, 1985; Vale *et al.*, 1985). In 1990 genes from *S. Cerevisiae* and *Aspergillus nidulans* were found to contain a region of ~350 amino acids which was 30-40% identical to the catalytic core of conventional kinesin, proving the existence of a kinesin superfamily. Each subfamily within the superfamily was found to contain a relatively well-conserved core motor domain linked to highly divergent non-motor domains, reflecting the functional diversity of their cellular roles. The structure of kinesin superfamily members is described in reference to that of the conventional kinesin heavy chain (KHC), which is the motor-contain polypeptide of the conventional kinesin holoenzyme.

Conventional Kinesin

The conventional kinesin holoenzyme is an elongated tetramer that consists of two heavy chains and two light chains (Cole and Scholey, 1995; Sablin, 2000) (Figure 2). The heavy chain of kinesin is comprised of four distinct regions; the catalytic core (amino acids 1-322), neck (amino acids 323-414), stalk (amino

Figure 2:
Conventional Kinesin Heavy Chain Domains

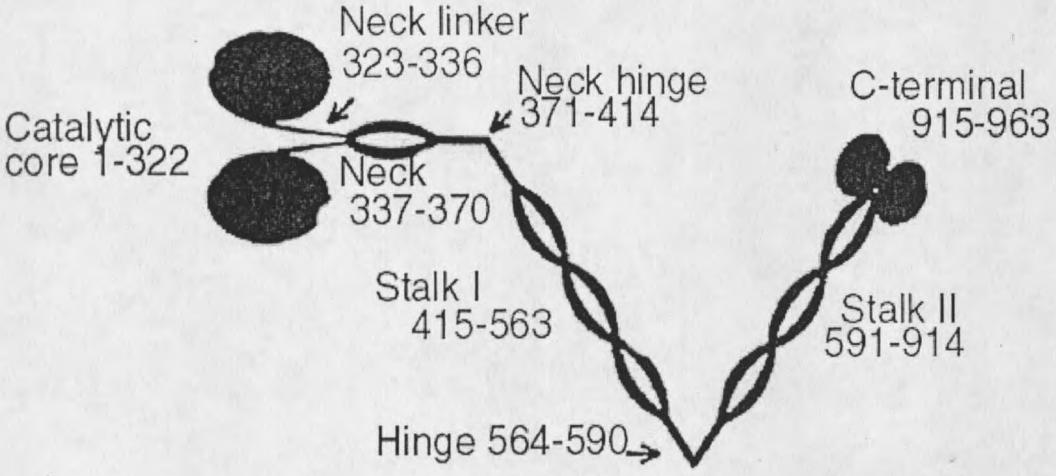


Figure 2:
Conventional kinesin heavy chain consists of four distinct regions; catalytic core, neck, stalk, and tail domains. The catalytic core is a globular domain, which includes the ~350 amino acid conserved region. The neck domain sequence is subfamily specific. It is divided into three regions; neck linker, coiled-coil, and hinge. The stalk domain forms two coiled-coils separated by a flexible hinge. The tail domain is globular and is thought to bind cargo.
(Pierce, D. 1999)

acids 415-914) and tail domains (amino acids 915-963). The catalytic core is a globular domain that generates force and binds ATP and microtubules. The kinesin superfamily may be divided into three main groups depending on position of the catalytic core within the polypeptide (Sablin, 2000). Kin C proteins are minus-end directed kinesins with the motor domain at the C-terminus, Kin N are plus-end directed and have N-terminal motor domains, and members of the Kin I have central (intermediate) motor domains and do not demonstrate traditional motor activity but may rather function as microtubule depolymerizing factors; their functions are still largely unknown (Desai *et al.*, 1999). My focus will be on the Kin N kinesins.

Adjacent to the catalytic core is the neck domain. This domain has been shown to be crucial to the mechanical functioning of the motor and determines movement direction (Case *et al.*, 2000). The first 10 amino acids of the neck are slightly conserved within all the Kin N motors and highly conserved within individual subfamilies. This region is termed the neck linker. Underlining its critical role in the movement mechanism, motor velocity decreases 200-500 fold when it is replaced with a random polypeptide sequence (Case *et al.*, 2000).

The neck linker is followed by a α-helical region made up of 20-30 residues. These amphipathic α-helices contain a heptad repeat $(abcdefg)_n$, where positions a and d are generally nonpolar amino acids (Thormahlen *et al.*, 1998). When these residues align a hydrophobic seam is generated along one side of the helix. When two amphipathic α-helices come in contact they wind around

another, interfacing hydrophobic/nonpolar residues, resulting in formation of a coiled-coil dimer. Dimerization of synthetic peptides corresponding to this part of the neck domain of a number of kinesins via coiled-coil formation has been proven via CD spectroscopic analysis (Tripet *et al.*, 1997). The neck coiled-coil region is conserved within subfamilies.

Recently, the Vale lab at UCSF discovered that by duplicating the first heptad repeat in the neck coiled-coil of K560, a construct from human conventional kinesin truncated at amino acid 560, the processivity of the motor increased by threefold (Romberg *et al.*, 1998). These results along with others confirm the necks involvement in motor function.

The neck linker and catalytic core combined are termed the "motor domain". The motor domain includes the ~350 amino acid conserved region mentioned earlier. Several crystal structures exist for kinesin motor domains including human conventional kinesin (Kull *et al.*, 1996), Drosophila Ncd (Sablin *et al.*, 1996), and rat conventional kinesin (Sack *et al.*, 1997) (Figure 3). Lower resolution crystal structures have also been obtained for conventional kinesin dimers (Kozielski *et al.*, 1997). The core motor domain consists of a central eight-stranded β-sheet sandwiched between six α-helices, three on either side. Comparison of myosin and kinesin crystal structures reveal that the larger myosin motor domain contains within its active site the same eight-stranded β-sheet sandwiched between six α-helices as conventional kinesin (Kull *et al.*, 1996; Rayment *et al.*, 1993). Within the motor domain there are several highly

conserved regions with distinct functions; including the P-loop, L12, L11 and Switch II α4-helix regions (Case *et al.*, 2000).

The P-loop participates in binding of the β and γ phosphates of ATP (Sack *et al.*, 1999). The Switch II α4-helix is involved in communication between the bound nucleotide and the MT binding site. These two regions are analogous to similar motifs in myosins and G proteins, which also share a similar fold. In G proteins the analogous region detects whether GTP or GDP is bound to the active site (Sack *et al.*, 1997). Depending on which form of the nucleotide is bound the switch region undergoes a conformational change. This initiates a chain reaction resulting in alterations in target protein binding affinity. The L12 region is the main MT binding site, although other regions contribute as well. This short highly conserved loop follows the Switch II α4-helix (Vale and Fletterick, 1997). L11 is a large 15 amino acid β-ribbon loop. It is directed away from the nucleotide-binding site and is thought to change its conformation during the ATP cycle.

There are three segments of (predicted) coiled-coil in conventional kinesin. Following the first region, in the neck domain, is a proline-glycine rich "hinge" region that separates the neck and stalk domains. The stalk domain is largely α-helical coiled-coil but is interrupted in the middle by another hinge. The stalk is not essential for motility, but does perform important functions. It acts as a spacer, conveys forces, and is responsible (along with the neck coiled-coil) for dimerization, which is the most common quaternary structure arrangement

among kinesins. Kinesin heavy chain dimerization is a result of the coiled-coil formation by the stalk and neck. The coiled-coils enable a kinesin heavy chain to bind with the corresponding region of its partner heavy chain, forming a long α-helical coiled-coil, which in turn forms a dimeric motor protein (Sack *et al.*, 1999).

The C-terminal end of the heavy chain folds to form a second globular region, termed the tail domain. Important differences among kinesins are found in this domain. The tail domain comes in various sizes, secondary structure and location with in the primary sequence. Like the stalk, the tail is not essential for motility but does perform other important functions. Since these two domains are not involved in motility they have not been studied as extensively as the head and neck domains. Hypotheses have been extended to the function of the tail for cargo binding, cargo regulation, and light chain binding (Cole and Scholey, 1995).

The light chain of KHC is involved in cargo binding and regulation (Cole and Scholey, 1995). It participates with the tail domain in the formation of a conformation of kinesin in which the tail domains fold back and interact with regions in the neck (and possible core) domains. In this conformation, the ATPase activity of the motor domains is inhibited (Verhey *et al.*, 1998). One hypothesis is the binding of cargo interferes with this head-tail interaction, releasing the motor domains and allowing kinesin to be motile. Transgenic mice lacking KHC displayed defects in axonal transport and other functions. Transgenic mice lacking kinesin light chains display the same defects, proving

light chains play an essential role in motor function (Rahman *et al.*, 1999). There are several light chain isoforms generated by alternative splicing, although their distinct functions have not been determined (Wedaman *et al.*, 1993).

Five motor quaternary configurations have been found: heterotetrameric ($\alpha_2\beta_2$), homotetrameric (α_4), homodimeric (α_2), heterotrimeric ($\alpha_2\beta$) and monomeric (α) (Figure 4). Movement is defined as either processive or multiple-motor nonprocessive. Processive movement occurs when an individual motor is able to translocate some distance along a microtubule. Multiple-motor nonprocessive movement is an additive effort made by many motors attached to a microtubule. Motor movement can be confirmed using microscopy or ATPase assays. Microtubule gliding and/or single molecule motility assays are used to visualize and quantitate microtubule velocity using differential interference contrast (DIC) or total internal reflection (TIR) microscopy. Three factors determine observed rates of motility in multiple motor gliding assays: (1) ATPase rate, (2) Step size, (3) Processivity or not. For processive motors, velocity is ATPase rate times step size. For nonprocessive, motors can make additive contributions to velocity, so observed velocity depends on how many motors are driving movement and is faster than the ATPase x step size. *In vitro* processive movement has only been observed for KHC and UNC104/KIF1 subfamily motors, although controversy exists as to whether the UNC104/KIF1 movement should be termed processive.

Figure 4:
Kinesin Superfamily Quaternary Structures

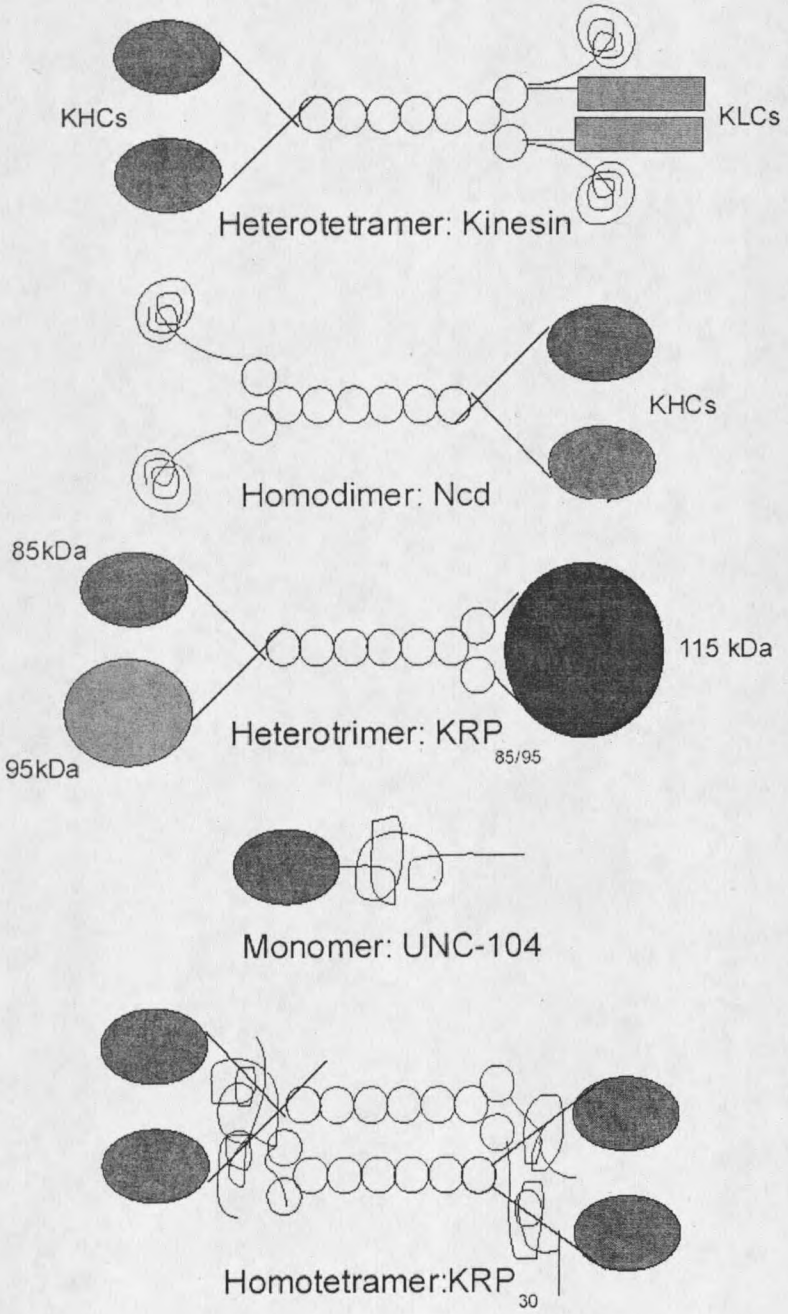


Figure 4: Quaternary Structures of the kinesin superfamily. Schematic depicts kinesin heavy chanins (KHCs) and kinesin light chains (KLCs). All kinesins are dimeric with the exception of the monomeric UNC104/KIF1 subfamiliy (Cole, *et.al.,* 1995).

In 1989 Howard, Hudspeth, and Vale discovered that dimeric conventional kinesin demonstrated processive movement *in vitro* (Vale and Toyoshima, 1989). It is hypothesized that the motor "walks" along the microtubule in a hand-over-hand fashion. This motion would rarely result in both motor domains detaching from the MT at the same time, thus maintaining a continuous connection between the motor and microtubule and preventing their otherwise rapid diffusional separtation. Conventional kinesin takes 8nm steps, each requiring the hydrolysis of one ATP. The first step of processive movement involves the binding of ATP to the leading head, Z. The ATP-bound state binds strongly to microtubules. Binding triggers docking of the neck linker domain on to the catalytic core, positioning the trailing head Y near its future binding site. Binding of Y to its new site causes it to release its bound ADP. The new trailing head (Z) then hydrolyzes its ATP and releases Pi. Since it now contains ADP, and the ADP state binds weakly to microtubules, it is now competent to release from the microtubule an move to its next binding site.

In previous studies members of the UNC104/KIF1 subfamily have not displayed processive movement in vitro, with one exception. A study from the Hirokawa lab reported processive movement of a monomeric KIF1A construct, C351 (Okada and Hirokawa, 2000). There is much speculation surrounding these results. The construct itself has the neck linker of conventional kinesin, a dimeric motor, and processive movement of constructs containing only KIF1A-derived sequence has not been reported. It is argued by the Hirokawa lab that

this addition is insufficient for dimerization and that it adds only stability to the KIF1A construct. Other members of the subfamily, which are not processive, have produced microtubule movement under multiple-motor conditions (Pierce *et al.*, 1999).

Conventional kinesin processive movement is a product the hand-over-hand motion of the two motor domains. This movement is made possible by the dimeric configuration of conventional kinesin. Dimerization of kinesin involves coiled-coil formation between the neck and stalk domains of the two motor heavy chains. Coiled-coil predictions of conventional kinesin show no coiled-coil formation in the motor domain followed by three large coiled-coil regions, one in the neck region and two in the stalk (Figure 5). When similar coiled-coil predictions are done for UNC-104, there is a notable decrease in coiled-coil formation (Figure 6). UNC-104 has no coiled-coil regions in the motor domain, followed by four smaller coiled-coils; one in the neck coiled-coil is found at ~360th amino acid, a second coiled-coil is found at ~400th amino acid, a third at ~600th amino acid, and finally a fourth smaller coiled-coil at ~800th amino acid. In accord with this low amount of predicted coiled-coil formation, KIF1A purified from native tissue or expressed heterologously was found to be monomeric (Okada Y., Hirokawa N., 1999) and the lack of *in vitro* processive movement, it was concluded that UNC104/KIF1 motors were monomeric.

Figure 5:
Coiled-coil Prediction of Conventional Kinesin

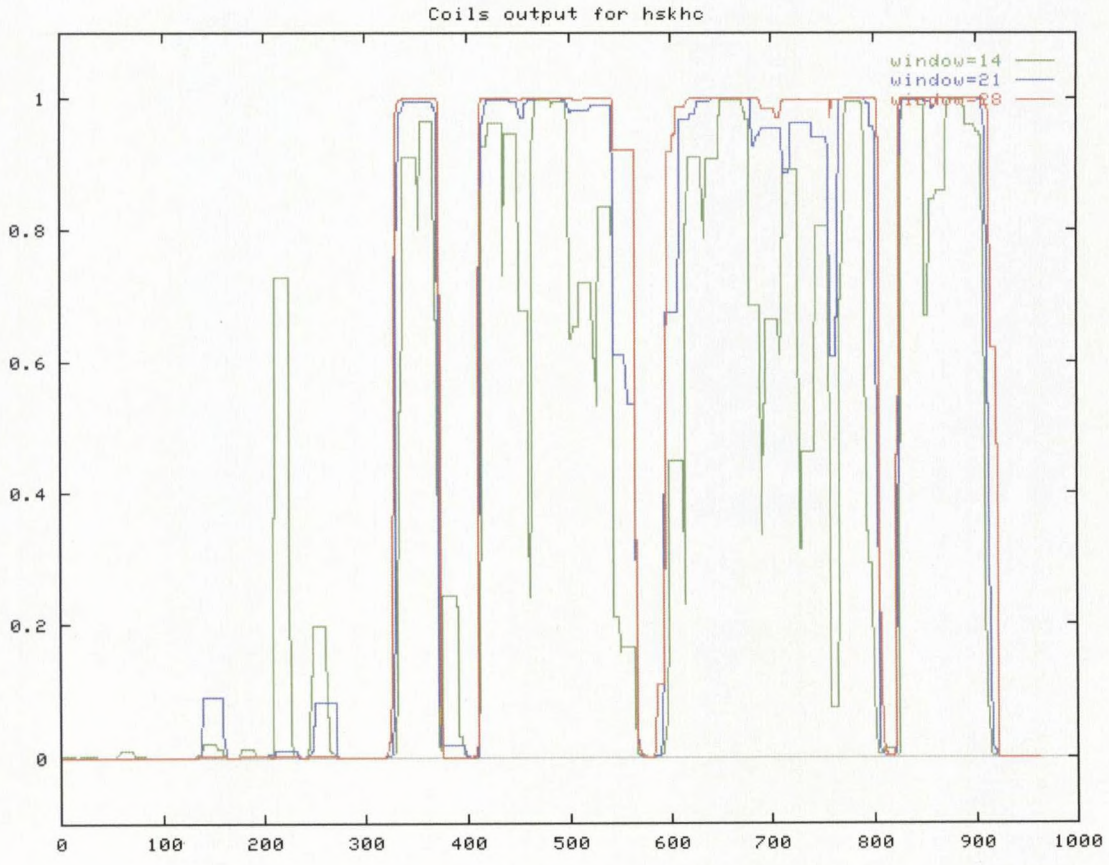


Figure 5:
Coiled-coil predictions in conventional kinesin. There are three frame widths present; windows 14, 21, and 28. Ability to form a coiled-coil was determined by analyzing the heptad repeat patterns within the amino acid sequence of HK560, a conventional kinesin truncation (Pierce D., 2000, unpublished results).

Figure 6:
Coiled-coil Prediction of UNC-104

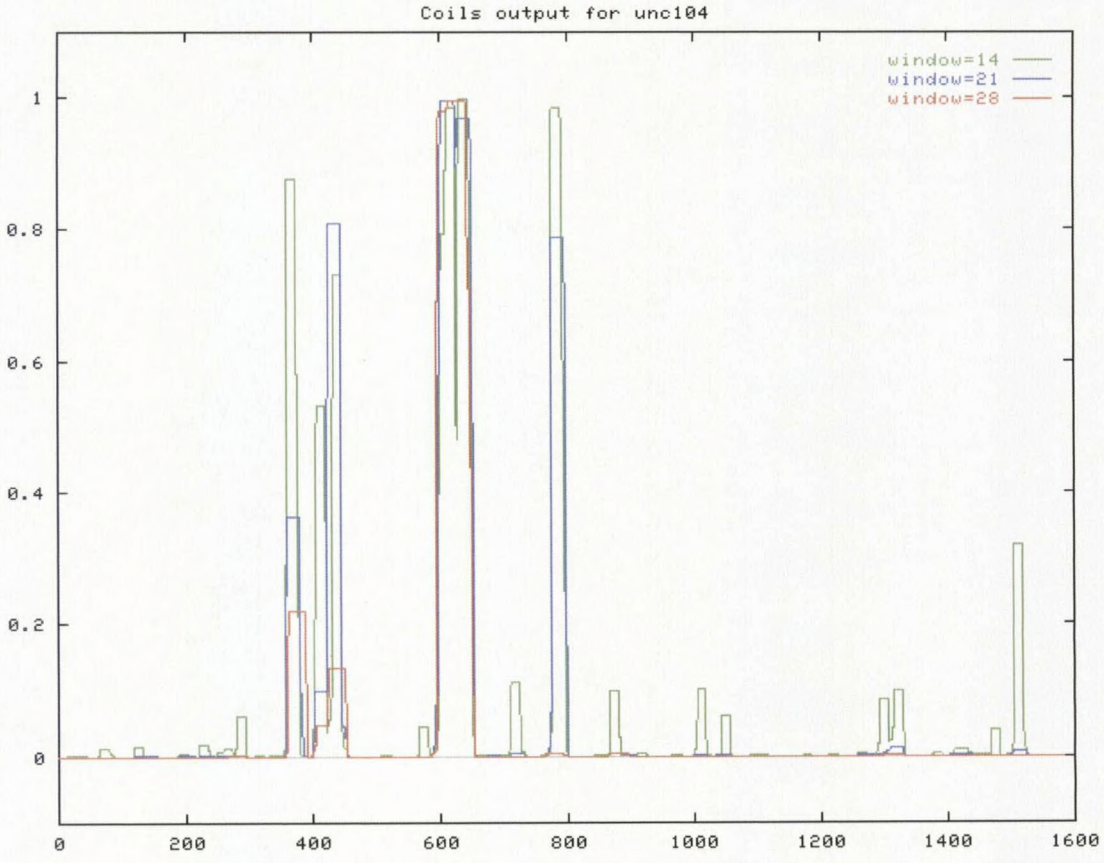


Figure 6:
Coiled-coil predictions in UNC-104. There are three frame widths present; windows 14, 21, and 28. Ability to form a coiled-coil was determined using the Lupas algorithm, whch detects heptad repeat patterns within the amino acid sequence of UNC-104 (Pierce D. 2000, unpublished results).

Monomeric Kinesin UNC104/KIF1 Subfamily

In microtubule gliding assays U653/GFP, a construct made from monomeric UNC-104, demonstrates a faster gliding velocity than conventional kinesin (Pierce *et al.*, 1999). The Vale lab reported a microtubule gliding velocity of 1760nm/sec and an ATP turnover rate of 5.5 ATPs per motor domain per second for U653/GFP (Pierce *et al.*, 1999). In contrast, HK560, a conventional kinesin construct, displayed a microtubule velocity of 402nm/sec and an ATP rate of 28 per motor per second, or 56 per dimer per second. It was concluded that the large differences between the monomeric and dimeric motors were most easily explained by position that with UNC-104 functions as part of a group many motors making additive contributions to the observed movement velocity. Most monomers are only attached to microtubules when actively involved in the power stroke portion of taking a step, unlike processive dimers, which are attached to the microtubule continuously for ~100 steps before diffusing away. This may decrease the organelle "drag" effect, which is apparent in dimers, thus allowing for increased motor velocities. It has also been proposed that monomeric motors move processively by an electrostatic tethering mechanism. KIF1 family motors are thought to utilize a strong positively charged lysine loop, that is conserved with in the subfamily for movement. Cryo-electron microscopy that was interpreted to support the hypothesis that there is an electrostatic interaction

between the lysine loop and the E-hooks, which are strongly negatively charged protrusion of glutamates on the α and β-tubulin subunits, of microtubules (Kikkawa *et al.*, 2000). This association occurs during the weak binding ATP state and allows the motor to diffuse along the microtubule. Another possibility involves a hypothesized lever arm, which could amplify the monomer's step size, thereby allowing rapid movement with a low ATP turnover rate. This theory suggests that monomeric kinesin and myosin motor movement is produced in a similar fashion. A third possibility that velocity enhancements could arise from nonprocessive additive movement involving lots of kinesins attached to the cargo taking steps larger than the 8nm/ATP of conventional kinesin. The latter two ideas are nonexclusive and were most consistant with available data (Pierce, *et. al.* 1999)

What parts of UNC-104 could comprise a long lever arm? UNC-104 contains tree coiled-coils, one of which is found in the neck domain. This domain has been previously linked to motor velocity in conventional kinesin (Case *et al.*, 2000). A lineup of the UNC104/KIF1 subfamily members shows a striking sequence similarity in the neck coiled-coil region, demonstrating its importance (Figure 7). After the coiled-coil region the sequences becomes divergent. The significance of the neck coiled-coil has generated an increased interest in UNC104/KIF1 motor structure and function. A recent study determined KIF1A neck coiled-coils had the highest probability of formation in native structure and were the most stable, even over conventional kinesin (B. Tripet and R. Hodges,

Figure 7:
UNC104/KIF1 Subfamily Coiled-coil Prediction

```
1          10         20         30         40         50
   KIF1A  LSTLRYADRA KQIRCNAIIN EDPNNKLIRE LKDEVTRLRD LLYAQGLGDI TDMTNALVGM
   KIF1B  LSTLRYADRA KQIKCNAVIN EDPNAKLVRE LKEEVTRLKD LLRAQGLGDI ID..TSMGSL
 HsKIF1C  LSTLRYADRT KQIRCNAIIN EDPNARLIRE LQEEVARLRE LLMAQGLSAS ALEGLKTEEG
CeUNC104  LSTLRYADRA KQIVCQAVVN EDPNAKLIRE LNEEVIKLRH ILKDKGIDV  TDVQETPGKH
 Dmkhc73  LSTLRYADRA KRIVNHAVVN EDPNARIIRE LRHEVETLRS MLKHATGSPV GDVQ......
DdUNC104  LSTLRYADSA KKIKTVAVVN EDAQSKLIRE LQGEVERLRA MMDQGGQYHA NDSKLMNSDY
           HELIX 6                cDefgAbc DefgAbcDef gAbcD
       <- Motor Core| Neck Linker |      Coiled-Coil       |
```

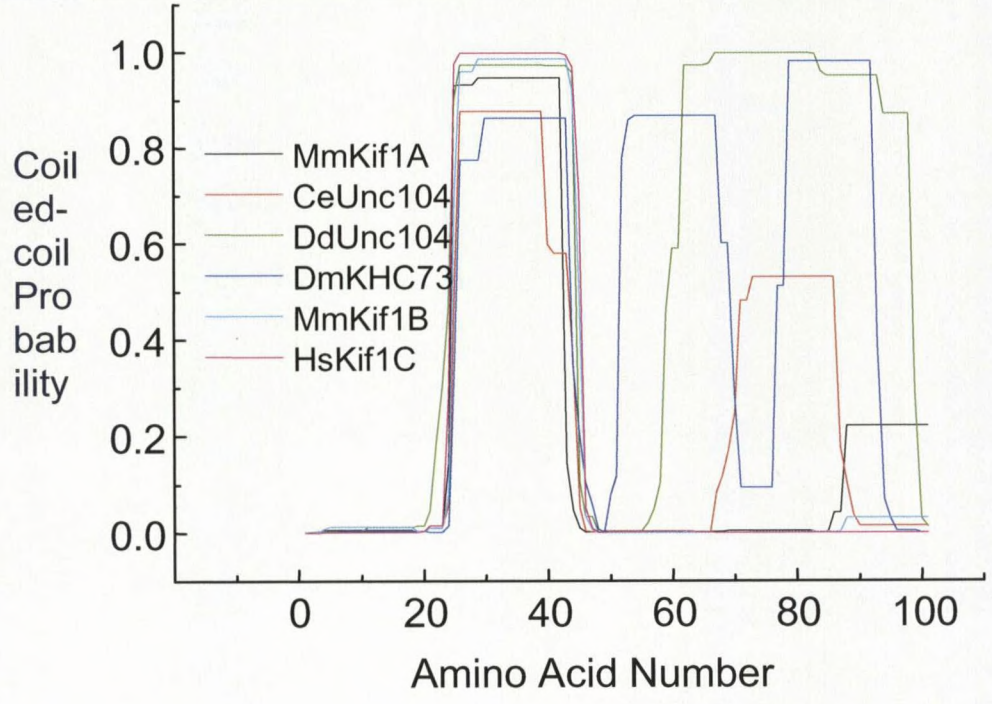


Figure 1.
Sequence lineup and coiled-coil probability of UNC-104 family motors. The lineup begins with and absolutely conserved motif (..lstl..) within helix six (blue text) of the core motor domain; many residues in this region are also conserved in the entire superfamily. The lysine at position 10 marks the end of superfamily conservation, and the ensuing neck linker and neck regions are conserved among subfamilies. The beginning and end points of the putative coiled-coil are shown in green, and its hydrophobic interface (a and d positions of the heptad repeat) are shown in red. The coiled-coil probability was predicted from the same beginning amino acid using the Lupas algorithm and a 7-amino-acid window size. Species listed are Mm, mus musculus, Ce, Caenorhabditis elegans, Dd, Dictyostelium discoideum, Dm, Drosophila melanogaster, and Hs, Homo sapiens (Pierce D. 2000, unpublished work).

personal communication). Due to the amphipathic nature of the neck α-helix, KIF1A would be unstable as a monomer. One way of reconciling these predicted coiled-coils with the data showing KIF1A and UNC-104 are monomers is to hypothesize that they form intramolecular coiled-coils, which could make a stiff, lever-like structure. Another possibility is that UNC104/KIF1 motors are actually dimers *in vivo* and the monomeric structure observed is an artifact of *in vitro* purification and assays. Two members of the subfamily, Ddunc104 and KIF1C, both motors are found as dimers in vitro (Dorner *et al.*, 1999; Pollock *et al.*, 1999). Ddunc104 is a motor protein found in the slime mold *Dictyostelium discoideum* and most closely resembles UNC-104. KIF1C is a kinesin-like motor found in mice and is involved in vesicle transport between the Golgi apparatus and the endoplasmic reticulum. KIF1C requires associated proteins in order to dimerize *in vitro*. It is plausible that all UNC104/KIF1A motors require associated cofactors for native configuration and function. In KIF1C, phosphorylation of serine 1092 allows for the association with the 14-3-3 proteins, initiating dimerization (Dorner *et al.*, 1999). The fork head associated (FHA), domain found in the neck region of UNC-104 may work in a similar fashion, regulating protein-protein interactions via phosphorylation (Westerholm-Parvinen *et al.*, 2000). The pleckstrin homology (PH), domain found at the COOH-terminus of UNC-104 and KIF1A, and regulates protein-protein interaction by phosphorylation (Gong *et al.*, 1999). Lastly, perhaps the binding of the motor or tail domain to a membrane-bound receptor brings two heavy chains closer,

triggering dimerization. Thus, although published data shows the purified proteins are monomers, whether members of the UNC104/KIF1A subfamily are monomeric or dimeric is nevertheless open to debate.

UNC-104 is a *C. elegans* neuronal motor protein. It is the orthologue of KIF1A, found in mice. UNC-104 and KIF1A are thought to translocate presynaptic vesicles down the axons. These vesicles contain neurotransmitters. When an action potential in the presynaptic cell reaches the axon terminal there is a rise in cytosolic Ca^{++}; the vesicles fuse with the plasma membrane, and release their contents into the synaptic cleft. The neurotransmitters diffuse across the cleft and fuse with postsynapic cell receptors.

UNC-104 contains a catalytic core similar to conventional kinesin, a neck linker and a short coiled-coil; the organization of the rest of the molecule is unknown. There are several subfamily -specific conserved regions in UNC104/KIF1A motors including the K-loop, PH, FHA, and neck coiled-coil conserved regions. In addition, an AF-6/CNO (canoe) region is conserved in the stalk domain of the monomers (Figure 8). The canoe protein is an effector for GTP-bound Ras. Ras plays an essential signaling role in regulation of various cell functions such as gene expression, cell growth, and generation and maintenance of the cytoskeleton. It interacts with the N-terminal of canoe and is postulated to control canoe's intracellular signaling. Because KIF1 motors contain a canoe region, it is possible they interact with and are regulated by Ras or a Ras-related molecule. The function of the conserved regions found in

Figure 8:
Conserved Regions in Monomeric UNC-104



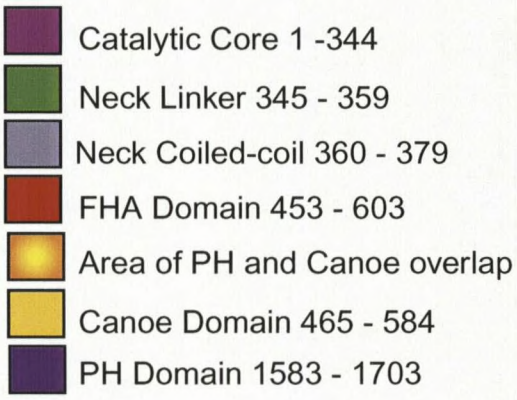


Figure 8:
Conserved regions found in the UNC-104/KIF1 subfamily .

monomeric motors is only speculative. There is, however, an established link between the neck region and motor velocity. This research addresses the suspected involvement of the neck coiled-coil in monomeric motor velocity. We were specifically interested in the possibility that an UNC-104 lever-arm could mediate its motility. Constructs were made to determine the effect of various neck truncations on the velocity of UNC-104.

CHAPTER 2

INTRODUCTION

The kinesin superfamily of microtubule-based motor proteins are involved in many cellular functions. Understanding the mechanisms by which kinesins generate force and movement is of both fundamental interest in cell biology and of therapeutic interest in medicine. Many motor proteins are essential for viability, as shown by the fatal nature of genetic lesions that abolish certain motor protein expression. Recent findings have demonstrated specific molecular linkages between kinesin superfamily motors and human diseases. Thus, advancement in the understanding of kinesin structure and function may provide beneficial information about disease pathology.

Recently, much attention has been focused on the role of the sequences that lie just outside the globular motor domain common to all kinesin superfamily members. The "neck linker" domain is immediately adjacent to the core motor domain, and current models place movements of this short segment of amino acids at the heart of the force generation mechanism. The neck linker is in turn adjacent to coiled-coil forming sequences that may function in both the force generating mechanism and in assembly and regulation of kinesin holoenzymes.

The UNC104/KIF1 or "monomeric" subfamily of kinesin motors have several interesting properties that indicate their movement mechanism may have some unique features. First, 8 of the 9 identified kinesin subfamilies contain two motor domains per holoenzyme, but the KIF1 family is believed to be monomeric, even though it contains sequences predicted to form coiled-coils. Second, the KIF1 family contains the fastest known kinesins, with measured movement velocities in the range of 2000 nm/sec. *in vitro*. These observations, together with the sequence features that are conserved among the KIF1 motors, have led me to test the possibility that KIF1 motors drive high-velocity movement by using a coiled-coil "lever-arm" that is different from and longer than the corresponding element in other kinesin motors, and that this structure allows them to travel a longer distance per ATP hydrolyzed.

To address the question of neck coiled-coil involvement in UNC-104 movement, I constructed and characterized three UNC-104 truncations. The truncation points were chosen so that the expressed constructs differed in which predicted coil-coil forming regions were present in the expressed construct. It was determined that deletion of neck coiled-coil had a modest effect on the microtubule velocities displayed by the UNC-104 constructs, thus, arguing against a lever-arm structure but not completely disproving its existence. Interestingly, the deletion of the neck linker domain in UNC-104 had a similar effect on motor velocity to that found in conventional kinesin, showing that, like

conventional kinesin the neck linker of UNC104/KIF1 motors is important for movement.

CHAPTER 3

MATERIALS AND METHODS

Plasmid Construction

All chemicals used are from Fisher Scientific unless indicated.

All constructs were made starting with a pET17b vector (Novagen Inc. Madison, WI) containing the N-terminal 653 amino acids of UNC-104 (U653), a kinesin-related protein, fused with Green Fluorescent Protein (GFP) tagged with a six histidine tag at its COOH-terminus. This construct was made by Daniel Pierce while in Ron Vale's lab at UCSF. The plasmids used in this study include; U345/GFP, U360/GFP, U380/GFP and U653/GFP. To create the desired truncations in the neck region of UNC104, fragments were PCR amplified using a Gibco 5'primer T7 (5'TAA TAC GAC TCA CTA TAG GG3') and MWG Biotech 3'primers encoded with a kpn1 restriction site (345; 5'GG GGG GGT ACC TTT CGC TCT ATC GGC ATA TCT CAA AGT3': 360; 5'CG CGC GGT ACC TTT TGC ATT TGG ATC CTC ATT AAC AAC3': 380; 5'CG CGC GGT ACC TCC CTT ATC TTT CAA AAT GTG ACG AAG3'). PCR amplification was performed using Stratagene native Pfu polymerase and an Eppendorf Mastercycler. U653/GFP fusion construct and PCR fragments were gel purified and extracted the using

GeneClean Extraction Kit (BIO 101, Carlsbad, CA). Fragments were then restriction enzyme digested with Xba1 (Promega) and Kpn1 (New England Bioscience) at 37^{0}C for 2 hours. The digested fragments were gel purified and extracted. The U653 portion of the U653/GFP fusion construct was replaced by subcloning in the PCR neck region truncation fragments and incubating with Takara T4 DNA ligase overnight at 16^{0}C. The resulting construct was then transformed into *Escherichia coli* DH5α competent cells and grown in Luria Bertani Broth (10g/L tryptone, 5g/L yeast extract, 10g/L NaCl, pH 7.0) with 100μM ampicillin overnight. Promega Wizard Plus Midi-preps were performed and the fusion protein DNA sequence was confirmed by dideoxy sequencing (Davis Sequencing, Davis, CA).

Protein Expression and Purification

All chemicals are from Fisher Scientific unless otherwise indicated.

Three protein preparations of each neck truncation were made. *Escherichia coli* BL21 (DE3) competent cells were transformed with the expression plasmid constructs. Colonies were selected and grown in 100mL of low salt TPM (20g/L tryptone, 15g/L yeast extract, 4g/L NaCl, 10mM glucose, 2g/L Na_2HPO_4, 1g/L KH_2PO_4, pH 7.0) with 100μg/mL ampicilian for 1 hour at 37^{0}C. The preculture was then inoculated into 900mL of low salt TPM media and grown at 37^{0}C to OD_{600} 0.6 – 0.8. The cells were then induced with 0.1mM isopropyl β-p-

thiogalactopyranoside (IPTG) and grown for an additional 18 hours at 22^{0}C to OD_{600} of 5.0 – 6.0. Cells were centrifuged at 8,000 rpm, 4^{0}C for 20 minutes and the pellets were stored at –80^{0}C.

Cells were resuspended in 25mL of lysis buffer (50mM NaPhos, 250mM NaCl, 1mM $MgCl_2$, 1mM ATP, pH 8.0). Then 10mM β-mercaptoethanol (βME), 20mM imidazole, 25μM PMSF (Sigma), 0.5 μg/mL leupeptin (Sigma), 0.5μg/mL aprotinin (Sigma), and 0.7 μg/mL pepstatin (Sigma) were added and the cells were lysed in a French Press at 12,000 – 14,000 psi. Insoluble material was removed by ultracentrifugation at 100,000 x g, 4^{0}C for 45 minutes. One mL of Ni^{2+} NTA resin (Qiagen Inc., Santa Clara, CA) was incubated with the supernatant on a roller at 4^{0}C for 45 minutes before the resin was transferred to a column. The Ni^{2+} NTA resin binds with the six-histidine tag of the UNC104/GFP truncated proteins.

Next, the Ni column was washed with 50mL of wash buffer (50mM NaPhos, 250mM NaCl, 1mM $MgCl_2$, 0.1mM ATP, 10mM BME, pH 6.0). One mL of elution buffer (50mM NaPhos, 250mM NaCl, 500mM imidazole, 1mM $MgCl_2$, 0.1mM ATP, 10mM BME, pH 7.2) was then applied and the resin was allowed to equilibrate 2-3 minutes. The protein was eluted with an additional 3mL of elution buffer and then diluted 10 fold with mono-S column buffer (25mM Pipes, 1mM DTT, 1mM EGTA, 1mM $MgCl_2$, 0.1mM ATP, pH 6.0). The protein was applied to a FPLC mono-S column (Pharmacia Biotech, Inc., Piscataway, NJ). Mono-S is a cationic affinity column bearing methyl sulfonate resulting in a negatively charged

matrix. After the protein was applied to the column, it was washed with column buffer. The column was eluted with a 0 to 1 M NaCl gradient. The kinesin-related protein eluted at ~0.35M NaCl. Protein concentrations were quantitated visually using SDS-PAGE 12% gels and a set of Bovine Serum Albumin (BSA) standards, which were stained with Coomassie stain. Immunoblotting was performed using a primary rabbit polyclonal anti-GFP antibody (from the Vale lab UCSF) and a secondary goat anti-rabbit IgG alkaline phosphatase conjugate (Sigma). It was determined that the mono-S fractions contained a GFP fusion protein the expected size of the designed U653/GFP fusion protein neck truncations, ~64kD. Peak fractions from the mono-S column were stored in liquid nitrogen after the addition of 10% sucrose.

Microtubule Affinity Purifications

All chemicals are from Fisher Scientific unless otherwise indicated.

Active motor proteins were isolated from the chromatographic fractions and the motor proteins concentrated using microtubule affinity purifications, also known as bind and release assays.

The concentration of 200µL of each motors mono-S fraction was determined by SDS-PAGE and comparison with BSA standards. An approximate four-fold molar excess of tubulin (Vale lab, UCSF) over motor was calculated. An appropriate amount of the 4.7mg/mL tubulin stock solution was pre-spun using a

Beckman tabletop ultra centrifuge at 100,000 rpm, 4^0C for 15 minutes with a TLA120.1 rotor to remove nonfunctional tubulin aggregates. The supernatant was removed and 0.5mM GTP and 20μM taxol (Sigma) was added to promote microtubule assembly and stability. The solution was then incubated at 37^0C for 5 minutes. The resulting polymerized microtubules were centrifuged through a cushion (12mM Pipes, 1mM EGTA, 1mM $MgCl_2$, pH 6.8 with KOH, and 60% v/v glycerol) in a Beckman tabletop ultra centrifuge at 80,000 rpm, 25^0C for 10 minutes in a TLA120.1 rotor. The cushion was washed with assay buffer (12mM Pipes, 1mM EGTA, 1mM $MgCl_2$, pH 6.8 with KOH) and 20μM taxol (Sigma) and the pellet resuspended in an assay buffer volume equal to $1/5^{th}$ the volume of tubulin stock solution used.

Two hundred μL of motor, 1mM AMP-PNP (Boehringer Mannheim), 200μL assay buffer, 20μM taxol and 20μL of microtubules were combined and incubated at room temperature for 15 minutes. AMP-PNP is a nonhydrolyzable ATP analogue that generates strong binding of most kinesin motors to microtubules. The solution was then spun over a cushion, as before. The resulting pellet was then resuspended in 100μL of release buffer (assay buffer supplemented with 200mM KCl, 5mM ATP, 5mM $MgCl_2$, and 20μM taxol and incubated at room temperature for 5 minutes. The solution was centrifuged at 80,000 rpm, 25^0C for 5 minutes in a TLA120.1 rotor, and the supernatant (containing the ATP-released motor proteins) was aliquotted and stored in liquid nitrogen after the addition of 10% sucrose. 12% SDS-PAGE gels were run to

determine the final protein concentration of the U653/GFP fusion protein truncations. A purity of approximately 50% active protein was found for each primary mono-S column fraction.

Microtubule Gliding Assays

All chemicals are from Fisher Scientific unless otherwise indicated.

Perfusion chamber construction

Perfusion chambers (flow cells) were made for MT gliding assays. Cover slips were washed with 25% HNO_3 for 10 minutes, rinsed twice with deionized water, washed with 2M NaOH for 10 minutes, rinsed six times with deionized water, and air-dried. Double-sided tape was used to space the dry acid washed cover slips away from and attach them to the slides. The flow cells each had a volume of ~4μL.

Generation of long microtubules

Frozen 4.7mg/mL tubulin (Vale lab, UCSF) was thawed quickly and centrifuged at 4^0C, 80,000 rpm in a TLA120.1 rotor for 15 minutes to remove tubulin aggregates. The supernatant was retained and the pellet discarded. Twelve μL of 100mM GTP and 100μL of DMSO was added per mL of tubulin

solution and incubated at 37^{0}C for 30 minutes. After 30 minutes 43μM of taxol (Sigma) was added to stabilize the microtubules. The polymerized MT's were then spun through 100μL of a cushion (60% v/v glycerol, 20μM taxol, 12mM Pipes, 1mM EGTA, 1mM $MgCl_2$, pH 6.8 with KOH) in a Beckman tabletop ultra centrifuge at 80,000 rpm, 25^{0}C for 10 minutes in a TLA120.1 rotor. The cushion and pellet were washed with assay buffer (12mM Pipes, 1mM EGTA, 1mM $MgCl_2$, pH 6.8 with KOH). 200μL of assay buffer and 40μM taxol (Sigma) was added per 1 mL of polymerized tubulin solution to the pellet with a P200 tip that had been cut-off (this prevents MT shearing). The pellet was gently resuspended and an equal volume of glycerol was added. The resulting solution was aliquotted into 20μL aliquots, frozen in liquid nitrogen, and stored at –80^{0}C.

Gliding Assays

Flow cells were filled with rabbit polyclonal anti-GFP antibody (Vale lab, UCSF) and the antibody was allowed to bind to the acid-washed coverslip surface for 2.5 minutes. The chamber was then washed with 50μL of BRB12 (12mM Pipes, 1mM EGTA, 1mM $MgCl_2$, pH 6.8 with KOH). Next, 5μL of MT affinity purified motor protein solution was flowed through the cell and allowed to bind to the antibody-coated surface for 2.5 minutes at room temperature (Figure 9). The chamber was once again washed with 50μL of BRB12 and 20mL of BRB12 containing 2mg/mL casein, 1mM ATP, 1mM DTT, 20μM taxol (Sigma)

Figure 9:
Kinesin Catalyzed Movement of Microtubules

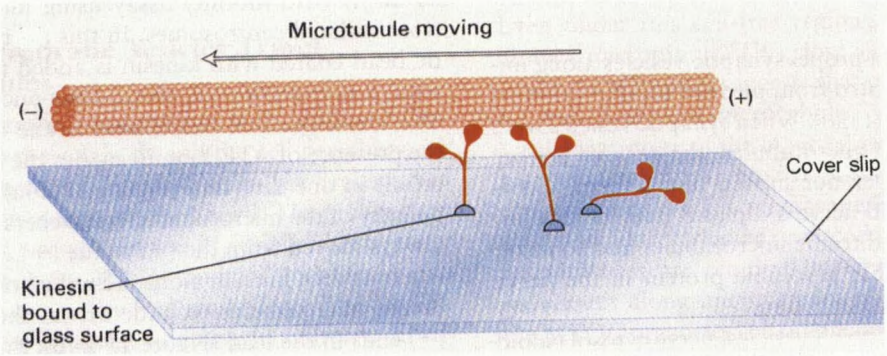


Figure 9:Kinesin motors are bound to an acid washed cover slip with an anti-GFP antibody coated surface. This immobolization results in the transmition of the sliding force from the motors to the microtubles, which then move in the direction of their negative ends. (Vale R., *et.al.*, 1985)

Figure 10:
DIC Image of Microtubules



Figure 10:
DIC microscopy provides a monochromatic shadow-cast image of organelles and macro-molecular complexes, such as MTs for in vitro motility assays. (http://www.blocks.fhere.org/%7Ekinesin)

and 1:400 dilution of MT's was flowed through. MT movement was recorded onto sVHS videotape using a TE300 Nikon microscope equipped with differential interference contrast optics (DIC). DIC imaging requires a 100W Hg lamp coupled with a fiber optic scrambler connected to an illumination pillar. The optical path consists of a polarizer, beam splitter, condenser, Wollaston prism, de Senarmont compensator, objective lens, Wollaston prism beam combiner, and an analyzer (Generation of image contrast, pg 89 – 91). DIC provides a monochromatic shadow-cast image of the microtubules (Figure 10).

MT velocities were determined using manually scoring the distances vs times of microtubule movement from videotape.

CHAPTER 4

RESULTS

Protein Expression and Purification

After some difficulties, expression and purification protocols were developed that yielded protein fractions with adequate purity and activity to permit their characterization in motility assays. The final concentrations were 0.05mg/mL-0.1mg/ml of the desired product (Figure 11). The fractions also contained varying amounts of degradation products but these were not harmful to the assays because they contained incomplete motor domains that do not interact with microtubules or have ATPase activity. Immunoblotting results proved the presence of GFP fusion proteins the expected size of each motor (Figure 12). Approximately 50% pure protein with a concentration of .025mg/mL–0.05mg/mL and better activity in microtubule gliding assays was obtained by microtubule affinity purification (Figure 13).

Figure 11:
Protein Purification SDS-PAGE Gels

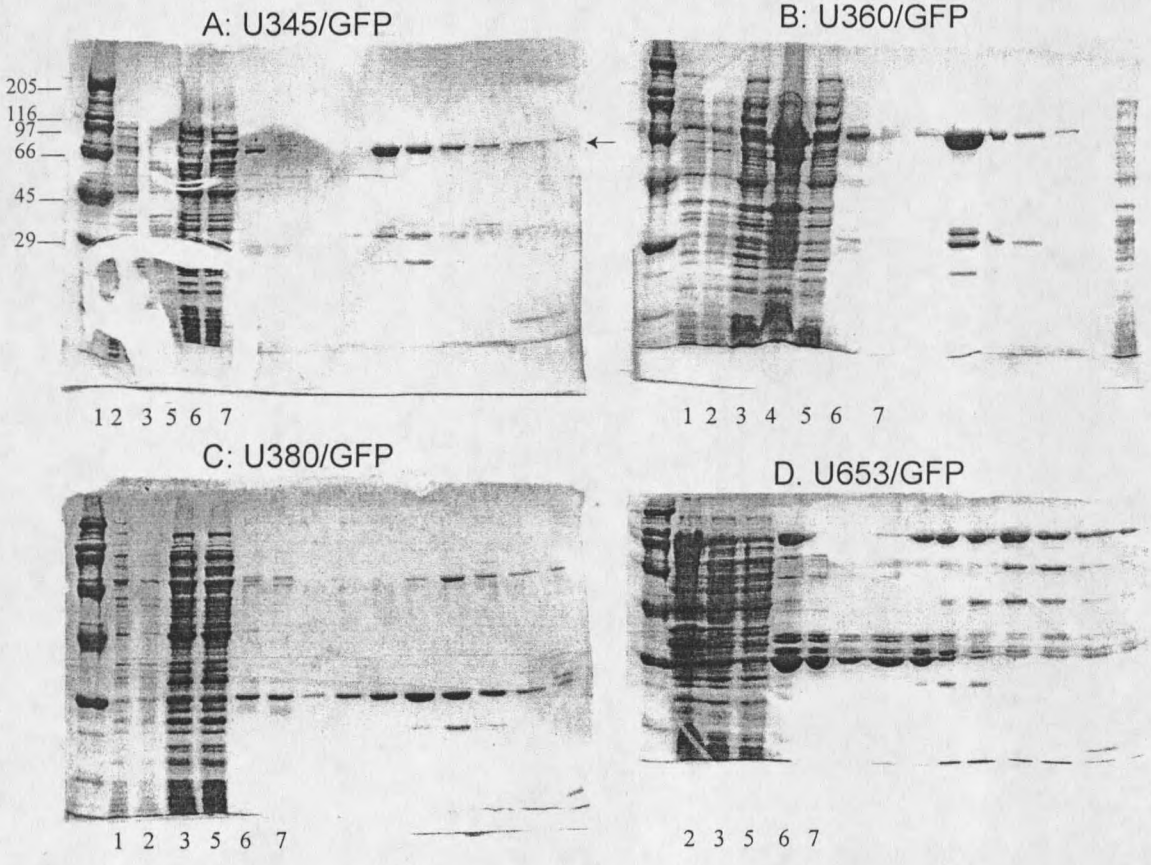


Figure 11: U345/, U360/, and U380/GFP purified recombinant proteins are ~64kD with concentrations between 0.1-0.05mg/mL. U653/GFP is ~110kD. (A) U345/GFP purification. (B) U360/GFP purification. (C)U380/GFP purification. (D) U653/GFP purification. Lane 1 for each gel corresponds to uninduced E. coli; lane 2 corresponds to IPTG-induced bacteria; lane 3 is the 100,000xg supernatant after French press lysis; lane 4 shows the 100,000xg French press pellet; lane 5 corresponds to the Ni eluate; lane 6 is the Ni flow through; and lane 7 is the Mono S flow through. Unmarked lanes are successive fractions from the Mono S column elution.

Figure 12:
Western Detection for GFP Fusion Protein

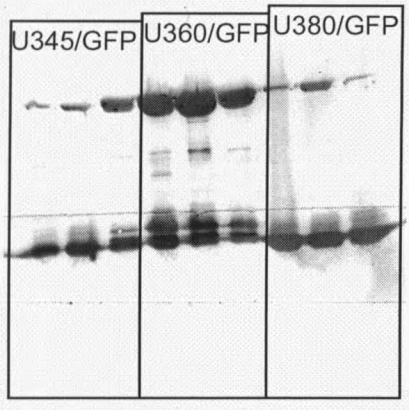
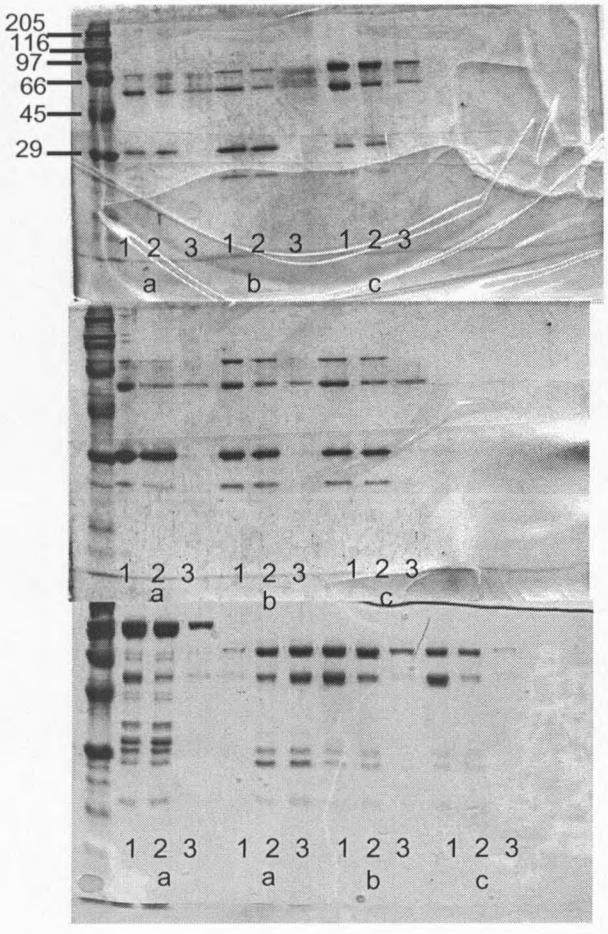


Figure 12: : Top bands are kinesin-GFP fusion protein, bottom bands are proteolyzed GFP. There are three separate protein purifications for each UNC-104 construct.

Figure 13:
Microtubule Affinity Purification SDS-PAGE Gels



A: U345/GFP

B: U380/GFP

C. U653/GFP U360/GFP

Figure 13: Microtubule affinity purification was performed on U345/, U360/, U380/, and U653/GFP. Column 1 is the protein and MTs before the assay began. Column 2 is the supernatant after the binding step (inactive protein is present). Column3 is the "active" protein after the release from the MTs. (a), (b) and (c) are the different protein preps,in order by date performed.

Microtubule Gliding Assays

The velocity of microtubule gliding driven by four different truncations of UNC-104-derived were quantitated and compared. At least two independent preparations of each protein were used for microtubule gliding assays. The longest construct, U653-GFP, had been previously characterized and found to produce a microtubule gliding velocity that is typical of this subfamily of motors and is probably equivalent to that of full-length UNC-104. Of the three shorter constructs described in this study, the two longer ones produced detectable microtubule gliding while the third did not. The velocity of microtubule movement for U360/GFP and U380/GFP found were 28 - 33% and 33 – 48%, respectively, of wild-type U653/GFP (Table 1, Figure 14) when assayed under the same conditions.

In this study, the U653/GFP displayed a velocity of 623+/-328nm/sec in BRB12, a low ionic strength solution containing 12mM K^+Pipes (Table 2, Figure 15). A previously published study with U653/GFP reported a velocity of 1760 nm/sec BRB80, which contains 80mM K^+Pipes but is otherwise identical (Pierce *et al.*, 1999). Lower ionic strength buffers generally cause microtubule gliding velocities to decrease, presumably due to increased electrostatic drag between the moving microtubule and surface-bound proteins. However, microtubules are

Table 1: Comparison of Various Neck Truncations on UNC-104 Velocity

Construct	Av. Velocity (nm/sec)	Standard Dev.
345-1/GFP	0	0
360-2/GFP	191	80
380-3/GFP	267	116
653/GFP	623	328

Table 1: Average velocity and standard deviation for each UNC-104 construct.

Figure 14:
UNC-104 Velocities Achieve with Various Neck Truncations

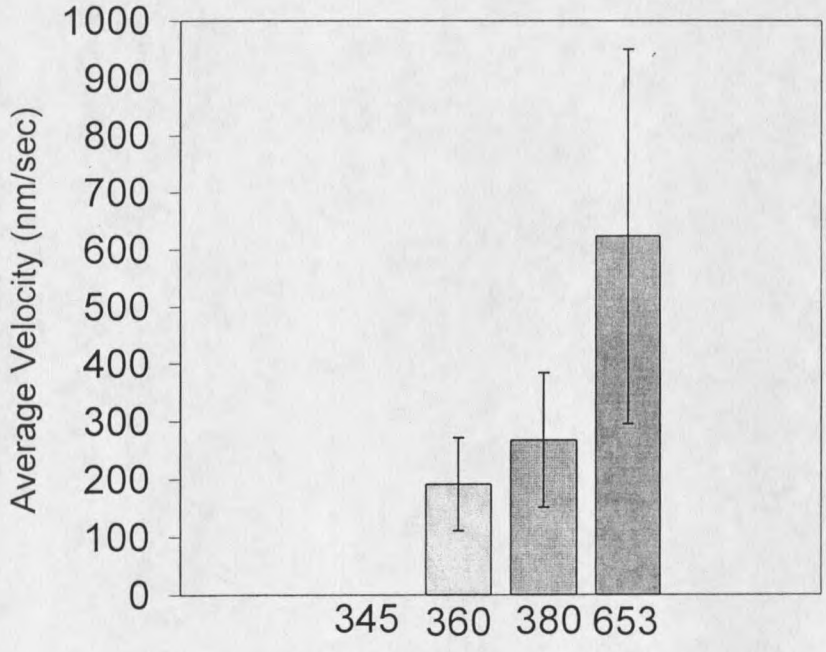


Figure 14: Average velocity of UNC-104 neck truncations with standard deviation.

Table 2: Velocities Displayed by U653/GFP

653/GFP
protein prep: 1/30/01
scope work: 03/26/01
score work: 03/28/01

tape: MK #2
time: 1.48.00 - 2.05.00
calibration: 0.02mm=14.2cm

No.	Total time (seconds)	Distance Moved (cm)	Conversion .01m=7.1cm		Velocity (mm/sec)
1	9	3.9	5.49E-03		6.10E-04
2	5	3.4	4.79E-03		9.58E-04
3	8	1.8	2.54E-03		3.17E-04
4	8	1.8	2.54E-03		3.17E-04
5	8	3.7	5.21E-03		6.51E-04
6	5	3	4.23E-03		8.45E-04
7	9	4.3	6.06E-03		6.73E-04
8	8	4	5.63E-03		7.04E-04
9	6	2.5	3.52E-03		5.87E-04
10	9	3.2	4.51E-03		5.01E-04
11	13	6.2	8.73E-03		6.72E-04
12	7	2.8	3.94E-03		5.63E-04
13	4	6	8.45E-03		2.11E-03
14	10	4	5.63E-03		5.63E-04
15	6	3	4.23E-03		7.04E-04
16	7	2.1	2.96E-03		4.23E-04
17	9	2.9	4.08E-03		4.54E-04
18	8	4.7	6.62E-03		8.27E-04
19	7	3.2	4.51E-03		6.44E-04
20	7	3.2	4.51E-03		6.44E-04
21	7	2.6	3.66E-03		5.23E-04
22	12	1.8	2.54E-03		2.11E-04
23	6	1.9	2.68E-03		4.46E-04
24	6	2.9	4.08E-03		6.81E-04
25	9	4.9	6.90E-03		7.67E-04
26	12	2.7	3.80E-03		3.17E-04
27	7	2.6	3.66E-03		5.23E-04
28	10	3.3	4.65E-03		4.65E-04
29	10	3.2	4.51E-03		4.51E-04
30	8	3.1	4.37E-03		5.46E-04

Average Vel.		6.23E-04
Standard Dev.		3.28E-04

Table 2: U653/GFP microtubule gliding velocities from 01/30/01 protein purification. See figure 15.

Figure 15:
Velocities Displayed by U653/GFP

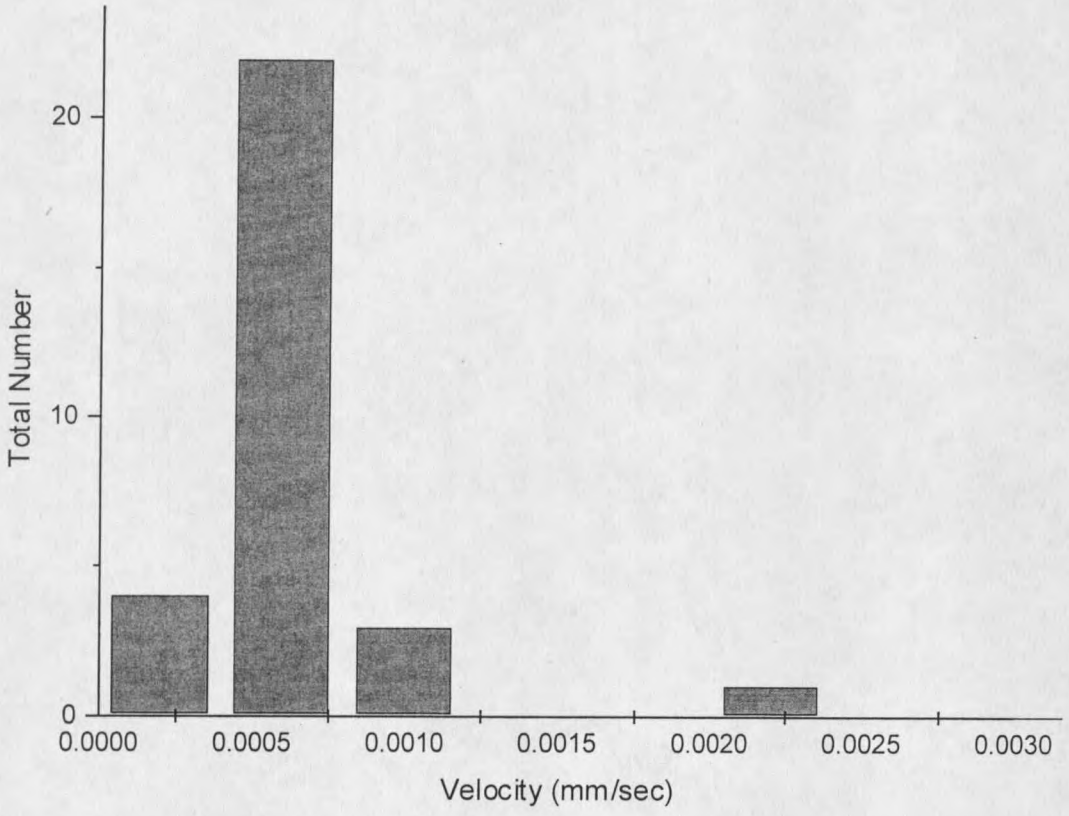


Figure 15:
Number of microtubules scored at each velocity.
Data is from one protein purification (See Table 2)

more efficiently retained on the surface at lower ionic strength, and use of BRB80 abolished microtubule gliding activity for the U360/GFP and U380/GFP constructs.

Although U345/GFP-coated surfaces efficiently bound microtubules, movement was not observed. In order to detect any slow movement that might be present, fields were imaged and recorded and then re-imaged after 60 minutes. Microtubule positions were compared to the positions of visible dust particles adsorbed to the cover slip to correct for any movement of the microscope stage during the 60 minute delay period. No microtubule movements were detected.

Microtubule affinity purified samples of U360/GFP and U380/GFP both gave rise to robust microtubule movement. The average gliding velocities were 192+/- 80nm/sec and 251+/- 116nm/sec, respectively, in BRB12 (Tables 3,4,5 and Figure16)(Tables 6, 7 and Figure 17). Although U380-GFP moved faster, the difference was not statistically significant.

Table 3: Velocities Displayed by U360/GFP

360-2/GFP
protein prep: 1/12/01
scope work: 03/26/01
score work: 03/28/01

tape: 360-2/GFP #2
time: 50.00 - 1.10.00
calibration: 0.02mm=14.2cm

No.	Total time (seconds)	Distance Moved (cm)	Conversion .01m=7.1cm		Velocity (mm/sec)
1	32	4.4	6.20E-03		1.94E-04
2	14	1.7	2.39E-03		1.71E-04
3	14	1.7	2.39E-03		1.71E-04
4	10	1.1	1.55E-03		1.55E-04
5	16	1.8	2.54E-03		1.58E-04
6	14	1.6	2.25E-03		1.61E-04
7	13	2.1	2.96E-03		2.28E-04
8	12	1.6	2.25E-03		1.88E-04
9	13	2.9	4.08E-03		3.14E-04
10	21	3	4.23E-03		2.01E-04
11	14	1.6	2.25E-03		1.61E-04
12	18	3.3	4.65E-03		2.58E-04
13	22	2.4	3.38E-03		1.54E-04
14	18	2.3	3.24E-03		1.80E-04
15	20	2.6	3.66E-03		1.83E-04
16	18	1.5	2.11E-03		1.17E-04
17	17	2.7	3.80E-03		2.24E-04
18	17	2.9	4.08E-03		2.40E-04
19	19	1.9	2.68E-03		1.41E-04
20	16	2.8	3.94E-03		2.46E-04
21	6	1.6	2.25E-03		3.76E-04
22	18	2.2	3.10E-03		1.72E-04
23	7	2.3	3.24E-03		4.63E-04
24	12	1.9	2.68E-03		2.23E-04
25	7	1.2	1.69E-03		2.41E-04
26	18	2	2.82E-03		1.56E-04
27	21	2.5	3.52E-03		1.68E-04
28	13	1.8	2.54E-03		1.95E-04
29	16	1.9	2.68E-03		1.67E-04
30	31	4.2	5.92E-03		1.91E-04

Average Vel.		2.07E-04
Standard Dev.		7.1701E-05

Table 3: U360/GFP microtubule gliding velocities from 01/12/01 protein purification. See figure 16.

Table 4: Velocities Displayed by U360/GFP.

360-2/GFP
protein prep: 1/22/01
scope work: 03/26/01
score work: 03/28/01

tape: 360-2/GFP #2
time: 1.10.00 - 1.30.00
calibration: 0.02mm=14.2cm

No.	Total time (seconds)	Distance Moved (cm)	Conversion .01m=7.1cm		Velocity (mm/sec)
1	19	2.2	3.10E-03		1.63E-04
2	20	1.4	1.97E-03		9.86E-05
3	20	1.2	1.69E-03		8.45E-05
4	30	2.9	4.08E-03		1.36E-04
5	30	5.4	7.61E-03		2.54E-04
6	13	2.6	3.66E-03		2.82E-04
7	17	1.9	2.68E-03		1.57E-04
8	12	2.2	3.10E-03		2.58E-04
9	12	1.8	2.54E-03		2.11E-04
10	20	3.1	4.37E-03		2.18E-04
11	20	2.3	3.24E-03		1.62E-04
12	9	2.1	2.96E-03		3.29E-04
13	37	4.7	6.62E-03		1.79E-04
14	20	2.9	4.08E-03		2.04E-04
15	18	2.4	3.38E-03		1.88E-04
16	22	3.3	4.65E-03		2.11E-04
17	34	1.6	2.25E-03		6.63E-05
18	21	2.9	4.08E-03		1.95E-04
19	28	2	2.82E-03		1.01E-04
20	14	2	2.82E-03		2.01E-04
21	29	3.7	5.21E-03		1.80E-04
22	13	1.9	2.68E-03		2.06E-04
23	34	4.5	6.34E-03		1.86E-04
24	34	2.6	3.66E-03		1.08E-04
25	24	1.6	2.25E-03		9.39E-05
26	46	2.1	2.96E-03		6.43E-05
27	29	2.5	3.52E-03		1.21E-04
28	14	1.9	2.68E-03		1.91E-04
29	11	2.1	2.96E-03		2.69E-04
30	20	2.1	2.96E-03		1.48E-04

Average Vel.		1.76E-04
Standard Dev.		6.57413E-05

Table 4: U360/GFP microtubule gliding velocities from 01/22/01 protein purification. See figure 16.

Table 5: Velocities Displayed by U360/GFP

360-2/GFP
protein prep: 1/25/01
scope work: 03/26/01
score work: 03/28/01

tape: 360-2/GFP #2
time: 1.30.00 - 1.50.00
calibration: 0.02mm=14.2cm

No.	Total time (seconds)	Distance Moved (cm)	Conversion .01m=7.1cm		Velocity (mm/sec)
1	15	3.1	4.37E-03		2.91E-04
2	22	3.6	5.07E-03		2.30E-04
3	23	2	2.82E-03		1.22E-04
4	58	2.6	3.66E-03		6.31E-05
5	16	2	2.82E-03		1.76E-04
6	31	5.2	7.32E-03		2.36E-04
7	56	2.1	2.96E-03		5.28E-05
8	26	3	4.23E-03		1.63E-04
9	22	4.5	6.34E-03		2.88E-04
10	12	1.3	1.83E-03		1.53E-04
11	18	3	4.23E-03		2.35E-04
12	36	3.1	4.37E-03		1.21E-04
13	17	3.3	4.65E-03		2.73E-04
14	21	4.2	5.92E-03		2.82E-04
15	14	3.1	4.37E-03		3.12E-04
16	25	1.4	1.97E-03		7.89E-05
17	29	6.2	8.73E-03		3.01E-04
18	48	2.3	3.24E-03		6.75E-05
19	48	2.7	3.80E-03		7.92E-05
20	56	2.2	3.10E-03		5.53E-05
21	8	2.1	2.96E-03		3.70E-04
22	41	6.1	8.59E-03		2.10E-04
23	8	2.3	3.24E-03		4.05E-04
24	26	2.8	3.94E-03		1.52E-04
25	15	2.1	2.96E-03		1.97E-04
26	20	1.8	2.54E-03		1.27E-04
27	13	2.6	3.66E-03		2.82E-04
28	25	4	5.63E-03		2.25E-04
29	22	2.1	2.96E-03		1.34E-04
30	36	2	2.82E-03		7.82E-05

Average Vel.		1.92E-04
Standard Dev.		9.86108E-05

Table 5: U360/GFP microtubule gliding velocities from 01/25/01 protein purification. See figure 16.

Figure 16:
Velocities Displayed by U360/GFP

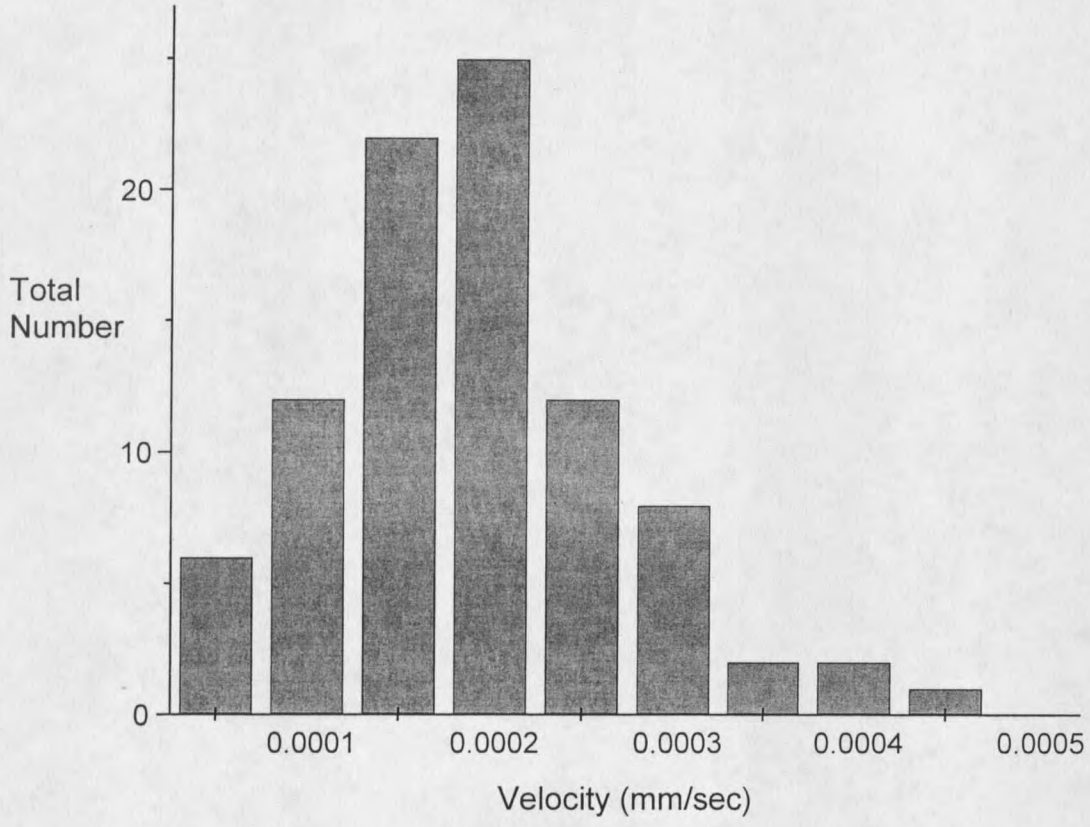


Figure 16:
Number of microtubules scored at each velocity. Data is from three separate protein purifications (See Tables 3, 4, and 5).

Table 6: Velocities Displayed by U380/GFP

380-3/GFP
protein prep: 1/23/01
scope work: 03/21 & 03/23
score work: 03/25/01

tape: 380-3/GFP
time: 1.00-11.00 & 1.45.00-2.05.00
calibration: 0.02mm=22.5cm

No.	Total time (seconds)	Distance Moved (cm)	Conversion .01m=11.25c		Velocity (mm/sec)
1	14	3.6	3.20E-03		2.29E-04
2	23	5.8	5.16E-03		2.24E-04
3	13	2.9	2.58E-03		1.98E-04
4	23	6.4	5.69E-03		2.47E-04
5	14	3.3	2.93E-03		2.10E-04
6	21	3.8	3.38E-03		1.61E-04
7	31	7.4	6.58E-03		2.12E-04
8	10	3.4	3.02E-03		3.02E-04
9	39	4.8	4.27E-03		1.09E-04
10	17	3.4	3.02E-03		1.78E-04
11	16	1.5	1.33E-03		8.33E-05
12	20	5.4	4.80E-03		2.40E-04
13	14	4.5	4.00E-03		2.86E-04
14	16	5	4.44E-03		2.78E-04
15	12	2.7	2.40E-03		2.00E-04
16	44	4.8	4.27E-03		9.70E-05
17	15	4.3	3.82E-03		2.55E-04
18	10	1.9	1.69E-03		1.69E-04
19	20	4.2	3.73E-03		1.87E-04
20	9	3.1	2.76E-03		3.06E-04
21	13	4.3	3.82E-03		2.94E-04
22	7	1.4	1.24E-03		1.78E-04
23	15	5.5	4.89E-03		3.26E-04
24	10	2.9	2.58E-03		2.58E-04
25	3	2.1	1.87E-03		6.22E-04
26	11	2.6	2.31E-03		2.10E-04
27	38	4.9	4.36E-03		1.15E-04

Average Vel.		2.06E-04
Standard Dev.		1.02E-04

Table 6: U380/GFP microtubule gliding velocities from 01/23/01 protein purification. See figure 17.

Table 7: Velocities Displayed by U380/GFP

380-3/GFP
protein prep: 1/26/01
scope work: 03/21/01
score work: 03/25/01

tape: 345-1/GFP
time: 2.00 - 31.00
calibration: 0.02mm=22.5cm

No.	Total time (seconds)	Distance Moved (cm)	Conversion .01m=11.25c		Velocity (mm/sec)
1	21	5.9	5.24E-03		2.50E-04
2	16	2.8	2.49E-03		1.56E-04
3	23	6.8	6.04E-03		2.63E-04
4	15	4.2	3.73E-03		2.49E-04
5	13	5.5	4.89E-03		3.76E-04
6	7	3.5	3.11E-03		4.44E-04
7	18	7.5	6.67E-03		3.70E-04
8	13	6.6	5.87E-03		4.51E-04
9	15	7	6.22E-03		4.15E-04
10	36	4.3	3.82E-03		1.06E-04
11	20	4.1	3.64E-03		1.82E-04
12	16	7.2	6.40E-03		4.00E-04
13	20	5.6	4.98E-03		2.49E-04
14	12	4	3.56E-03		2.96E-04
15	14	3.6	3.20E-03		2.29E-04
16	10	3.9	3.47E-03		3.47E-04
17	16	5.4	4.80E-03		3.00E-04
18	32	4.8	4.27E-03		1.33E-04
19	15	4.2	3.73E-03		2.49E-04
20	10	4.6	4.09E-03		4.09E-04
21	9	6.7	5.96E-03		6.62E-04
22	19	6.7	5.96E-03		3.13E-04
23	16	7.1	6.31E-03		3.94E-04
24	23	6.2	5.51E-03		2.40E-04
25	19	7.6	6.76E-03		3.56E-04
26	16	3.9	3.47E-03		2.17E-04
27	24	4.7	4.18E-03		1.74E-04
28	19	5.5	4.89E-03		2.57E-04
29	10	4.5	4.00E-03		4.00E-04
30	22	3.8	3.38E-03		1.54E-04

Average Vel.		3.01E-04
Standard Dev.		1.19E-04

Table 7: U380/GFP microtubule gliding velocities from 01/26/01 protein purification. See figure 17.

Figure 17:
Velocities Displayed by U380/GFP

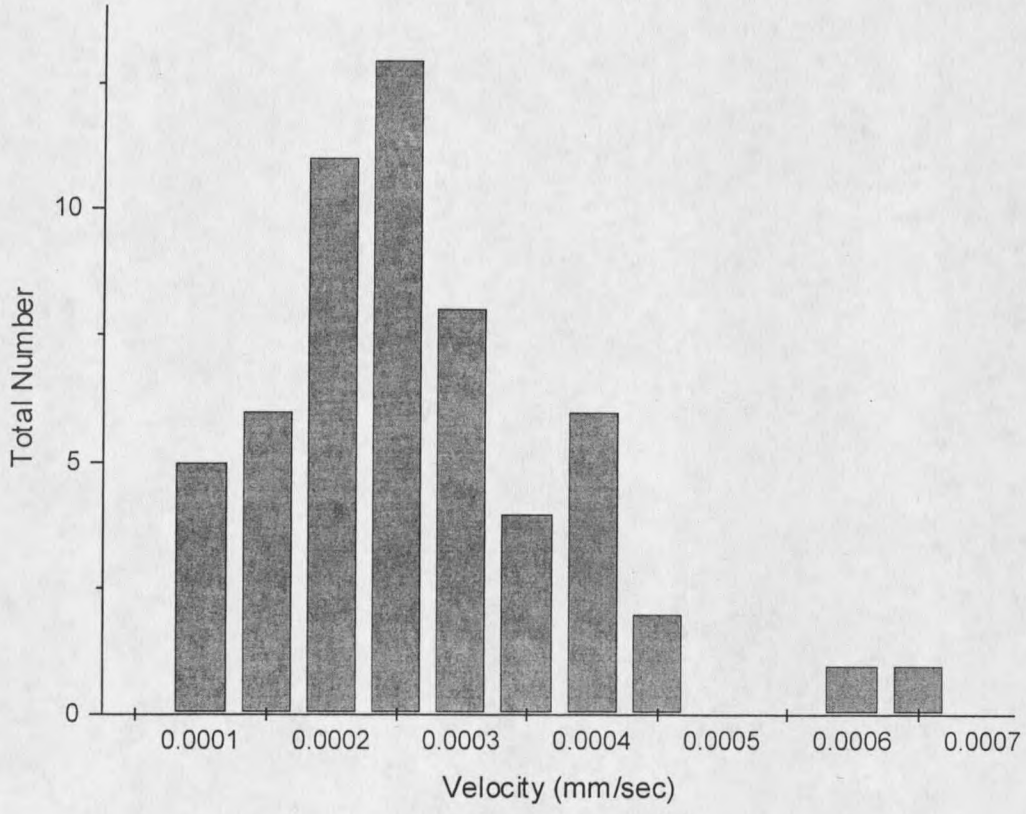


Figure 17:
Number of microtubules scored at each velocity. Data is from two separate protein purifications (See Tables 6 and 7).

CHAPTER 5

DISCUSSION

The UNC-104/KIF1 subfamily of kinesins are unique in two respects: first, they produce very high rates of microtubule gliding, and second, their predicted structure does not contain the long α-helical coiled-coil "stalk" domains found in other kinesins. In accord with their sequence characteristics, studies of UNC-104 family motors to date have found that *C. elegans* UNC-104 and its murine orthologue KIF1A are monomeric when purified from native tissues or heterologously expressed, while the *Dictyostelium* motor DdUnc-104 and murine KIF1C contain more predicted coiled-coil and are dimers.

Conventional kinesin is a processive enzyme that can take hundreds of 8-nm steps along a microtubule without dissociating by using its two motor domains in an alternating, hand-over-hand fashion. Monomeric motors cannot utilize this processivity mechanism. Accordingly, UNC-104 and KIF1A do not move processively. Although KIF1A has been reported to exhibit long-distance biased diffusional movement, this mechanism is fundamentally different than that of conventional kinesin and an individual motor utilizing this mechanism cannot exert a sustained force against a load.

The behavior of processive vs. non-processive motors in multiple-motor filament gliding assays is quite distinct. For processive motors such as conventional kinesin that maintain continuous contact with the microtubule, the microtubule can only translocate as fast as is allowed by the slowest motor with which it is interacting. Since the motors execute their mechanical cycles stochastically, increasing the number of motors driving transport results in mechanical drag from excess attached motors and decreased velocity. In the absence of a mechanical load on the microtubule, the fastest movement is obtained when a single motor drives transport. In contrast, for non-processive motors such as muscle myosin, no transport of actin filaments is observed when only a single myosin interacts with the filament. Since each myosin interacts with the actin filament for only part of its cycle, multiple motors make (up to a point) additive contributions to the observed movement velocity. In practice the observed velocities are fairly constant over a broad range of surface densities. In a simple model, the observed maximal velocity is equal to the step size times the ATPase rate divided by the percentage of its cycle that the motor spends bound to the filament (the duty cycle). For example, a processive motor that produces a 10nm step per ATP and hydrolyzes 10 ATP's per second would produce a velocity of 100nm/s (duty cycle of one). 10 non-processive motors with the same step size and ATPase rates, but a duty cycle of 0.1, could collectively produce a filament velocity of 1000nm/s.

Processive motors are constrained to take steps that correspond to the underlying periodicity of the filament (8nm in the case of microtubule motors); non-processive motors are not similarly constrained. Since UNC-104 is not processive, we speculated that it may utilize both a low duty cycle and a large step size to produce the fast observed movement velocities. The step size of (non-processive) myosins has been shown to result from movement of a mechanical amplified (or "lever arm") through a fixed angular displacement (Spudich, 1994); thus, increasing the length of the lever-arm increases the step size. The central question addressed in this work is if UNC-104 works in a similar manner. Although it is a monomer, UNC-104 contains coiled-coil forming sequences. Since coiled-coils can form elongated, mechanically stiff structures, we speculated that UNC-104 may contain intramolecular coiled-coils that act as a lever arm to increase the UNC-104 step size. Alternatively, UNC-104 may achieve high velocities using the same kind of movement of the neck linker that has been proposed for conventional kinesin (and that produces a moderate step size) coupled with a low duty cycle and a fast ATPase rate.

Three truncated versions of UNC-104; U345/GFP, U360/GFP, and U380/GFP, were cloned, expressed, purified, and characterized to distinguish among these possibilities (Figure 18). A predicted coiled-coil occurs between residues 360 and 380, so comparison of U360/GFP and U380/GFP should be informative as to any mechanical functions of this sequence. The role(s) of additional coiled-coil after residue 380 can be evaluated by comparing U380/GFP

Figure 18:
Schematic of UNC-104 Constructs

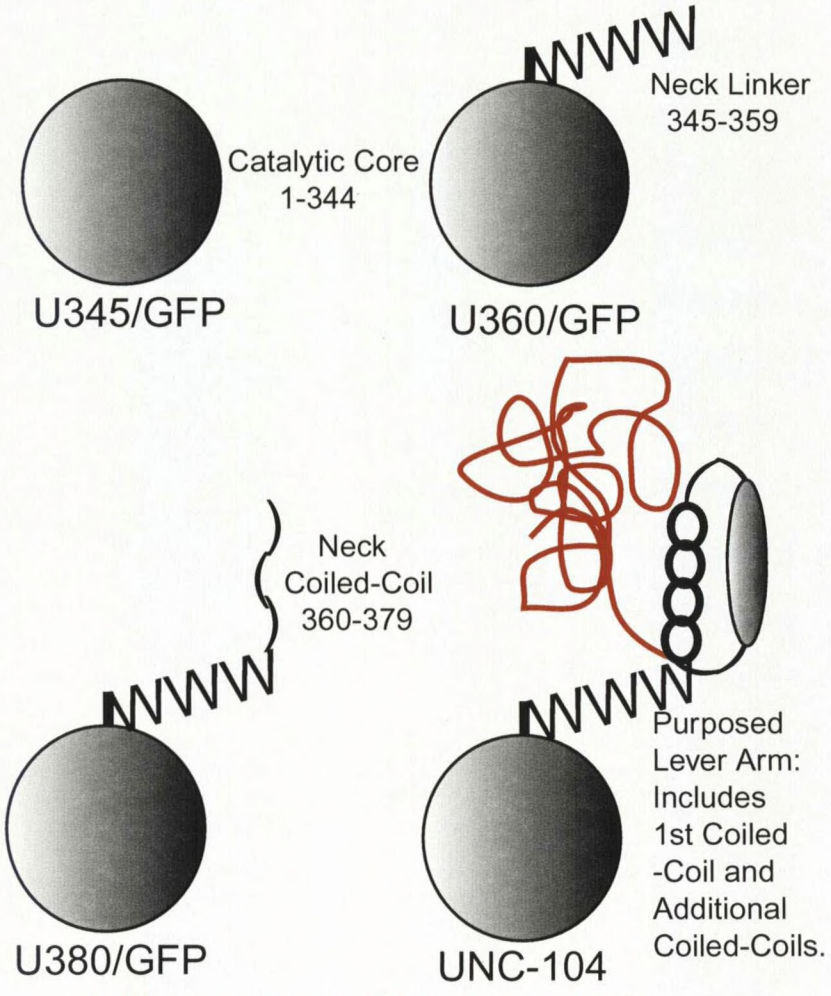


Figure 18:
Schematic of UNC-104 constructs with various neck truncations.

to the (pre-existing) U653/GFP construct. Finally, the U345/GFP construct deletes the neck linker domain. If the UNC-104 and conventional kinesin mechanisms are similar, we would expect a very large difference in motility properties between U345/GFP and U360/GFP by analogy to similar constructs of conventional kinesin. To allow for a common method of surface adsorption of the constructs in microtubule gliding assays and to allow for future experiments involving total internal reflection (TIR) microscopy, each construct was fused C-terminally to the Ser65Thr mutant of green fluorescence protein (GFP).

Amino acid 345 is a highly conserved lysine throughout the kinesin superfamily. This truncation occurs just before the neck linker and corresponds to amino acid 323 in human kinesin. U360/GFP included the first 360 NH_2-terminal amino acids of UNC-104, followed by a Kpn1 restriction site and GFP. Amino acid 360 a lysine that is highly conserved among the Unc-104 subfamily motors and immediately precedes the neck coiled-coil domain. Thus the U360/GFP construct includes the neck linker, with the sequence terminating before the neck coiled-coil. U380/GFP includes the first 380 NH2-terminal amino acids of UNC-104, followed by a Kpn1 restriction site, ending with GFP. U380/GFP ends at the COOH-terminus of the neck coiled-coil. Amino acid 380 is only slightly conserved. In UNC-104 amino acid 380 is an isoleucine.

Both U360/GFP and U380/GFP were found to be functional motors. They displayed the ability to glide microtubules under multiple-motor conditions, bind to microtubules in the presence of AMP·PNP, and release from microtubules in the

presence of ATP. U345/GFP produced no microtubule gliding under multiple-motor conditions, although it had the capability of microtubule binding while in the presence of AMP·PNP, and was able to release in the presence of ATP. Thus it is unlikely that the motor was nonfunctional during gliding assays due to an inability of the protein to fold properly.

The data obtained in this study argues against the lever-arm model for UNC-104 movement. I have shown that neck truncations at amino acids 360 and 380, before and after the first coiled-coil, respectively, resulted in similar velocities, and the velocities obtained with either construct are only modestly less than that obtained with U653/GFP. However, the complete lack of movement obtained with U345/GFP indicates that the neck linker region is essential for motility, and its presence is sufficient to produce rapid microtubule movement. Thus it appears likely that force generation by UNC-104 family motors is based on structural rearrangements very similar to those proposed for conventional kinesin (Rice *et al.*, 1999).

Two questions are of particular interest for future studies. The first is, what is the step size produced by UNC-104? This question is best addressed by optical trapping microscopy. The second is, if the coiled-coil segments found in Unc-104 do not function as a lever arm, what is their function? The highly conserved nature of these sequences argues strongly that they are functionally important. It is my view that these sequences, perhaps in concert with other polypeptides, mediate formation of an UNC-104 holoenzyme that contains two motor domains

and that the physiologically relevant complexes of UNC-104 family motors are structurally more similar to other kinesins than has been proposed based on *in vitro* studies performed to date.

Other experiments which would assist in the clarification of UNC-104 structure include; sucrose density gradient assays, ATPase assays, single-molecule motility assays, and assays performed with motor proteins purified from native tissues.

Sucrose density gradient assays would determine the molecular weight of each construct. From this information it could be concluded if the motors are functioning as monomers or dimers *in vitro*. Using this technique the Vale lab at UCSF has reported U653/GFP is a monomer *in vitro* (Pierce *et al.*, 1999).

ATPase assays and single-molecule motility assays would address the conflicting issue of processivity in the UNC104/KIF1A subfamily. In the Vale lab it was found that U653/GFP was not processive in both single-molecule motility assays and ATPase assays (Pierce *et al.*, 1999). The Hirokawa lab in Japan produced a KIF1A construct (C351), which displayed biased diffusional movement, which they termed "processive" even though this mechanism clearly is quite different from that of conventional kinesin (Okada and Hirokawa, 1999).

In vivo assays or *in vitro* assays with motors purified under mild conditions from native tissues would be invaluable. These studies could resolve the debate on monomeric verses dimeric configuration in UNC104/KIF1A motors. If native tissue were used, there would be an increased likelihood of cofactors involved in

motor assembly and/or activity being present, giving a more accurate representation of the motor *in vivo*.

With the procedures performed, it was concluded that truncations before and after the neck coiled-coil had little, if any, influence on motor velocity. In contrast, a truncation made before the neck linker had a severe effect. Instead of supporting the theory of a lever-arm in UNC-104, my research argued against it. Since they argue against one alternative hypothesis as to the function of the neck coiled-coil domain, my results could be indirectly interpreted in support of the idea that native UNC104/KIF1 motors function as dimers, not monomers, in the cell. However, since microtubule gliding velocity differences between different constructs can only be interpreted semi-quantitatively, this study does not disprove the lever-arm theory completely.

CHAPTER 6

SUMMARY

There is much debate involving monomeric motor protein motility. Studies with conventional kinesin have shown that the neck region, in particular the neck linker, is involved in motor velocity. The question of how motility is performed in monomeric motors remains unanswered. It is theorized that monomeric motor movement is mediated by a lever-arm protruding from the motor. There are multiple conserved regions within the UNC104/KIF1 subfamily, starting in the neck and continuing to the COOH-terminus. These regions are thought to play an integral role in structure and/or function of the motor. The neck coiled-coil is highly conserved within the subfamily, it could possibly be involved in an internal coiled-coil, forming the stiff lever-arm. My research focused on the neck region of UNC-104. I wanted to determine if the neck coiled-coil was important for motor motility velocity. My results proved that there is little, if any, effect on motor velocity with the deletion of the coiled-coil, arguing against, but not disproving, the lever-arm theory. It was also determined that deletion of the neck linker had a severe effect on motor motility, similar to that found in conventional kinesin. Conclusions could be drawn from these results implicating that UNC104/KIF1 motors are dimeric in the cell.

CHAPTER 7

REFERENCES CITED

1. Brady, S. T. (1985). A novel brain ATPase with properties expected for the fast axonal transport motor. *Nature* **317,** 73-75.

2. Case, R. B., Rice, S., Hart, C. L., Ly, B., and Vale, R. D. (2000). Role of the kinesin neck linker and catalytic core in microtubule-based motility. *Current Biology* **10,** 157-160.

3. Cole, D. G., and Scholey, J. M. (1995). Structural variations among the kinesins. *Trends Cell Biol.* **5,** 259-262.

4. Desai, A., Verma, S., Mitchison, T. J., and Walczak, C. E. (1999). Kin I kinesins are microtubule-destabilizing enzymes. *Cell* **96,** 69-78.

5. Dorner, C., Ullrich, A., Haring, H.-U., and Lammers, R. (1999). The kinesin-like protein KIF1C occurs in intact cells as a dimer and associtates with proteins of the 14-3-3 family. *The Journal of Biological Chemistry* **274,** 33654-33660.

6. Dupuis, L., de Tapia, M., Rene, F., Lutz-Bucher, B., Gordon, J. W., Mercken, L., Pradier, L., and Loeffler, J.-P. (2000). Differential screening of mutated SOD1 transgenic mice reveals early up-regulation of a fast axonal transport component in spinal cord motor neurons. *Neurobiology of Disease* **7,** 274-285.

7. Goldstein, L. S. (1993). With apologies to Scheherazade: tails of 1001 kinesin motors. *Ann. Rev. Genetics* **27,** 319-351.

8. Gong, T.-W. L., Winnicki, R. S., Kohrman, D. C., and Lomax, M. I. (1999). A novel mouse kinesin of the UNC-104/KIF1 subfamily encoded by the Kif1b gene. *Gene* **239,** 117-127.

9. Hoenger, A., Sack, S., Thormahlen, M., Marx, A., Muller, J., Gross, H., and Mandelkow, E. (1998). Image reconstructions of microtubules decorated with monomeric and dimeric kinesins: comparison with x-ray structure and implications for motility. *J Cell Biol* **141,** 419-430.

10. Kikkawa, M., Okada, Y., and Hirokawa, N. (2000). 15 angstrom resolution model of the monomeric kinesin motor, KIF1A. *Cell* **100**.

11. Kozielski, F., Sack, S., Marx, A., Thormahlen, M., Schonbrunn, E., Biou, V., Thompson, A., Mandelkow, E. M., and Mandelkow, E. (1997). The crystal structure of dimeric kinesin and implications for microtubule-dependent motility. *Cell* **91,** 985-994.

12. Kull, F. J., Sablin, E. P., Lau, R., Fletterick, R. J., and Vale, R. D. (1996). Crystal structure of the kinesin motor domain reveals a structural similarity to myosin. *Nature* **380,** 550-555.

13. McDonald, H. B., Stewart, R. J., and Goldstein, L. S. (1990). The kinesin-like ncd protein of Drosophila is a minus end-directed microtubule motor. *Cell* **63,** 1159-1165.

14. Okada, Y., and Hirokawa, N. (1999). A Processive Single-Headed Motor: Kinesin Superfamily Protein KIF1A. *Science* **283,** 1152-1157.

15. Okada, Y., and Hirokawa, N. (2000). Mechanism of the single-headed processivity: diffusional anchoring between the K-loop of kinesin and the C terminus of tubulin. *Proceedings of the National Academy of Sciences* **97,** 640-645.

16. Pierce, D. W., Hom-Booher, N., Otsuka, A. J., and Vale, R. D. (1999). Single molecule behavior of monomeric and heteromeric kinesins. *Biochemistry* **38,** 5412-5421.

17. Pollock, N., de Hostos, E. L., Turck, C. W., and Vale, R. D. (1999). Reconstitution of membrane transport powered by a novel dimeric kinesin motor of the Unc104/ KIF1A family purified from Dictyostelium. *The Journal of Cell Biology* **147,** 493-505.

18. Rahman, A., Kamal, A., Roberts, E. A., and Goldstein, L. S. (1999). Defective kinesin heavy chain behavior in mouse kinesin light chain mutants. *Journal of Cell Biology* **146,** 1277-1288.

19. Rayment, I., Rypniewski, W. R., Schmidt-Base, K., Smith, R., Tomchick, D. R., Benning, M. M., Winkelmann, D. A., Wesenberg, G., and Holden, H. M. (1993). Three-dimensional structure of myosin subfragment-1: a molecular motor. *Science* **261,** 50-58.

20. Rice, S., Lin, A. W., Safer, D., Hart, C. L., Naber, N., Carragher, B. O., Cain, S. M., Pechatnikova, E., Wilson-Kubalek, E. M., Whittaker, M., Pate, E., Cooke, R., Taylor, E. W., Milligan, R. A., and Vale, R. D. (1999). A structural change in the kinesin motor protein that drives motility. *Nature* **402,** 778-784.

21. Romberg, L., Pierce, D. W., and Vale, R. D. (1998). Role of the kinesin neck region in processive microtubule-based motility. *J Cell Biol* **140,** 1407-1416.

22. Sablin, E. P. (2000). Kinesins and microtubules: their structures and motor mechanisms. *Current Opinion in Cell Biology* **12,** 35-41.

23. Sablin, E. P., Kull, F. J., Cooke, R., Vale, R. D., and Fletterick, R. J. (1996). Crystal structure of the motor domain of the kinesin-related motor ncd. *Nature* **380,** 555-559.

24. Sack, S., Kull, F. J., and Mandelkow, E. (1999). Motor proteins of the kinesin family. Structures, variations, and nucleotide binding sites. *Eur. J. Biochem.* **262,** 1-11.

25. Sack, S., Muller, J., Marx, A., Thormahlen, M., Mandelkow, E. M., Brady, S. T., and Mandelkow, E. (1997). X-ray structure of motor and neck domains from rat brain kinesin. *Biochemistry* **36,** 16155-16165.

26. Scholey, J. M., Porter, M. E., Grissom, P. M., and McIntosh, J. R. (1985). Identification of kinesin in sea urchin eggs, and evidence for its localization in the mitotic spindle. *Nature* **318,** 483-6.

27. Spudich, J. A. (1994). How molecular motors work. *Nature* **372,** 515-518.

28. Thormahlen, M., Marx, A., Muller, S. A., Song, Y., Mandelkow, E. M., Aebi, U., and Mandelkow, E. (1998). Interaction of monomeric and dimeric kinesin with microtubules. *J Mol Biol* **275,** 795-809.

29. Tripet, B., Vale, R. D., and Hodges, R. S. (1997). Demonstration of coiled-coil interactions within the kinesin neck region using synthetic peptides. Implications for motor activity. *J. Biol. Chem.* **272,** 8946-8956.

30. Vale, R. D., and Fletterick, R. J. (1997). The design plan of kinesin motors. *Annu. Rev. Cell Dev. Biol.* **13,** 745-777.

31. Vale, R. D., Schnapp, B. J., Mitchison, T., Reese, T. S., and Sheetz, M. P. (1985). Kinesin: a novel microtubule-based force generating protein. *In* "Microtubules and Microtubule Inhibitors" (M. DeBrabander and J. DeMey, Eds.), Vol. 3, pp. 213-224. Elsevier Press.

32. Vale, R. D., and Toyoshima, Y. Y. (1989). Microtubule translocation properties of intact and proteolytically digested dyneins from *Tetrahymena* cilia. *J. Cell Biol.* **108,** 2327-2334.

33. Verhey, K. J., Lizotte, D. L., Abramson, T., Barenboim, L., Schnapp, B. J., and Rapoport, T. A. (1998). Light chain-dependent regulation of kinesin's interaction with microtubules. *The Journal of Cell Biology* **143,** 1053-066.

34. Wang, J., Yu, W., and Baas, P. W. (1996). Microtubule assemb ly in growing dendrites. *Journal of Neuroscience* **16,** 6065-6078.

35. Wedaman, K. P., Knight, A. E., Kendrick, J. J., and Scholey, J. M. (1993). Sequences of sea urchin kinesin light chain isoforms. *J Mol Biol* **231,** 155-8.

36. Westerholm-Parvinen, A., Vernos, I., and Serrano, L. (2000). Kinesin subfamily UNC104 contains a FHA domain: boundaries and physicochemical characterization. *FEBS Letters* **486,** 285-290.

MONTANA STATE UNIVERSITY - BOZEMAN
3 1762 10350782 6